Core-shell, ultra-small particles, monoliths and other support materials in high performance liquid chromatography

Nobuo Tanaka, GL Sciences Inc., Iruma, Saitama 358-0032 Japan.

n-tanaka@gls.co.jp

David.V. McCalley, Centre for Research in Biosciences, University of the West of England, Frenchay, Bristol BS16 1QY, U.K.

David.Mccalley@uwe.ac.uk

1. Introduction

Considerable developments have taken place in the area of supports for high performance liquid chromatography (HPLC) over the last ten years or so since the commercial introduction of smaller sub-2 μm particle columns[1]. These particles offer particular advantages in terms of increasing the speed of analysis, which is of paramount importance when large numbers of samples must be analysed. Shorter analysis times, particularly in conjunction with the use of columns of smaller internal diameter, offer considerable savings in the cost of mobile phase solvents and their disposal. Small superficially porous "core shell" or simply "shell" materials have gained considerable popularity in recent years and advances in methods of preparation, performance and comparison with totally porous particle columns will be a feature of this review. The review will cover the use of very small particles in capillary column formats to determine their potential compared with the use of columns of more conventional diameters (1- 4.6 mm ID), particularly with the objective of increasing the detection sensitivity when combined with mass spectrometry.

The review will include the improvements that have been made in the preparation and performance of monolithic columns. These columns have important differences from particle packed columns, and their current status in comparison with advanced particulate columns will be considered. There are also significant differences in the preparation and performance of "rod" columns (with similar dimensions to conventional HPLC columns) and capillary monoliths, which will be considered. While the review will concentrate on monolithic silica materials, proposed around twenty years ago and later commercialised by Merck[2], the most recent developments in organic polymer and with hybrid silica-organic polymer columns, will also be included.

New types of support material have continued to be developed such as pillar array columns, which in some cases can rival the performance of conventional particle packed columns[3]. Recent progress in this area will be included.

The work will mostly cover publications in 2012-2015, but will also include important earlier papers that may assist in the appreciation of the significance of these new developments. While relatively few fundamental advances have occurred in the area of support materials over the last few years, much has been contributed in research aimed at increasing our understanding of their performance, which bodes well for the enhancement of the properties of these materials in the future. Thorughout, the review will concentrate on the support materials themselves, rather than on the stationary phases that result from bonding different ligands, or from other manipulations of the supports. Special mention should be made of the extensive work in all areas of the review, by the late Professor Georges Guiochon, who sadly passed away in October 2014[4-6].

2 Small particle/shell particle columns.

2.1 General considerations

While the potential advantage of small particles had been recognised for many years[7], particularly with regard to their capabilities for fast analysis, their practical implementation in commercial systems has not been realised until relatively recently. Besides the requirement for higher pressure and lower dead volume equipment in order to realise their full performance[8], problems can arise due to frictional heating effects and shifts in retention that can be caused as a consequence of high pressure operation[9]. Further major innovations have taken place with the introduction of superficially porous particles or "core-shell" phases in which a porous layer of stationary phase surrounds a non-porous core that is impervious to solute penetration.

While shell particles have been used in liquid chromatography for nearly fifty years with larger "pellicular" particles of diameters in the region of 50 μm[10], the concept has only relatively recently been introduced for use with small particles of smaller (2.7 μm) diameter[11]. The newly developed material had in addition, a value of ρ, the ratio of the diameter of the solid core divided by the diameter of the whole particle of ~0.63 compared with a figure close to 1.0 for the

original pellicular particles. Thus, these new particles can be regarded as having a thick shell, as compared with the thin shells of the earlier particle design and therefore should be much less prone to overloading effects than the original particles.

The advantage of these newer shell columns is that they can give efficiencies very similar to that of sub 2μm totally porous particles while generating pressures of around half or less[12]. It is important to realise that the flow resistance of shell and totally porous particles of the same diameter is about the same whether the bead is porous or non-porous, because the pore diameter is too small relative to the interstitial space to allow flow through the pores[13]. The advantage of shell particles is thus due to smaller plate heights compared with totally porous particles of the same size; alternatively larger shell particles can be used at lower pressure to generate the same performance. The considerable decrease in required pressure as particle size increases results from the pressure drop on the column being inversely proportional to the square of the particle diameter[14]. The advantages of core-shell materials may result in some way from their narrow particle size distribution (psd), although this is a subject of much debate; fully porous materials with an improved psd have also been prepared in order to explore the possible benefits of this approach[15] .

The practical application of shell particles has recently been briefly reviewed[16]. It was concluded that shell particle technologies are continuing to expand in their applications to small molecule separations through the introduction of alternative surface chemistries and a widened assortment of particle sizes. Materials with wider pore structures have recently been made available that allow larger molecules such as peptides and proteins to be separated. A substantial list of the different stationary phase chemistries available, and a listing of many applications of these materials has also been given[17].

2.2 Core-shell particles. Methods of Preparation.

Shell particles are now available from all the major column manufacturers. These particles appear to have few drawbacks. While the total surface area of the column packing is naturally reduced by the presence of the solid core, the (usually small) reduction in retention and loading capacity

that results does not appear problematic[18]. Overloading of these particles will depend on the physical dimensions of the particle, but does not usually present difficulties (see below). Thus, research has continued to optimise their methods of preparation.

The very great majority of both totally porous and shell particles continue to be made from silica. Many variants of the process to produce shell particles exist[13] and have been recently extensively reviewed, so will not be covered again in detail here. The most popular procedure involves the initial synthesis of micrometer sized, non-porous silica cores, typically using the Stoeber process[19]. The porous shell is built up by a layer- by- layer approach. The negatively charged core particles are first treated with a positively charged organic polymer which is held to the core by electrostatic and other forces. Excess of this material is removed by rinsing and filtration or centrifugation. This is followed by coating with a suspension of silica nanoparticles typically of particle siz (d_p) of 10-16 nm, of opposite charge. The process is repeated until the desired shell thickness is achieved. According to Chen et al., 5-6 coatings must be applied to achieve a layer 0.25 μm thick[20] and 40-50 coats for a 0.5 μm shell. An alternative procedure, the one step coacervation procedure first developed by Kirkland,[21] is to apply a polymer to the cores that can absorb several layers of sol particles, such that the porous shell grows 5-10 layers at a time. However, >10 coating steps are still needed to achieve a 0.5 μm thick shell. Subsequently, a new coacervation procedure where the surface modified solid silica spheres are suspended in a mixture of urea, formaldehyde and colloidal silica under acid conditions has been developed[20]. The core is first modified with a material that has similar chemical properties to the urea /formaldehyde polymer e.g. ureidopropyltrimethoxysilane. The polymer is finally removed by burning and the particles are sintered at high temperature. The various steps in these procedures are illustrated in Fig. 1.

Another one pot synthesis is based on the “sphere on sphere process”. This type of particle has been applied to the fast HPLC separation of peptides and proteins[22-25]. Modification of the Stöber method with tetraethyl orthosilicate (TEOS) as the silica precursor and adding polyvinyl alcohol plus cetyltrimethylammonium bromide lead to the production of monodisperse, porous silica

microspheres. If mercaptopropyltrimethoxysilane is used in place of TEOS, silica microspheres are produced with a single layer of nanospheres coating the surface and are described as "sphere-on-sphere" particles. The one-pot reaction, removes the need for time-consuming preparation and classification steps. The particles were functionalised with C4 and used in 10 x 0.21 cm columns, shown to give comparable separations of a standard peptide mixture and a protein mixture consisting of solutes of 6-670 kDa to a classical core shell column of similar dimensions packed with 2.6 μm particles. When analysed using nitrogen adsorption, SOS particles have been shown to be microporous, with pore diameter <2 nm. However, while the surface of the material might not exhibit significant porosity, when packed into a column the spaces between the surface nanospheres provide superficial macroporosity. Further improvement in the performance of these materials might be obtained by size classification, although this did not appear to be necessary due to the narrow psd and good performance shown in the applications.

Materials other than silica have, however sometimes been used to construct the core or shell. For example, Deng and Marlow developed a method to coat polystyrene particles with an organo-silicone shell, although these materials seem designed for applications outside HPLC such as in medicine or catalysis, where core-shell materials have also attracted considerable attention[26]. Hung et al synthesised carbon core particles derived from oxidised and carbonised polystyrene-divinylbenzene particles, in order to prepare materials that might overcome the pH and temperature instability of silica[27]. They used layer- by- layer deposition of amine containing polymer and nanodiamond onto these carbon cores, and subsequent functionalisation of the particles. The particles showed good mechanical, thermal and pH stability, and good separations of essential oils were demonstrated. A commercially available variant of this material with pore size 180 Å was independently evaluated for the separation of proteins. As the stationary phase contains some protonated amine groups within the structure, the retention mechanism was expected to be a mixture of hydrophobic interaction and anion exchange, although it appeared the former was the dominant mechanism[28]. The robustness of the material allowed the effect of temperature variation over the range 30-80 ^{o}C to be studied even with the use of larger amounts of TFA than usual (0.2-0.5%) compared with the usual 0.05-0.1 %), which was necessary to

improve efficiency. Changing the temperature over this range hardly affected the peak capacity of the gradient separations, but did give interesting selectivity changes. Wide pore 120, 180 and 250 Å materials of this type were again evaluated for the separation of proteins[29]. The largest pore size gave the best performance for large molecules. The particles were shown to be smooth, (see Fig. 2) and therefore do not benefit from the proposed packing advantages of rough silica particles, a property which may improve the radial homogeneity of the packing and reduce eddy dispersion. However, it was considered that eddy diffusion may not be a significant contributor to band broadening for large molecules, and the particle morphology might even improve mass transfer.

2.3 Performance of columns packed with shell, totally porous and non-porous particles.

2.3.1 Effect of particle size and column dimensions.

The advantages of smaller fully porous particles compared with the same materials in conventional larger particles sizes can be clearly demonstrated by kinetic plots as shown in Fig. 3 (a)[30] . The pressure limit of the conventional columns (used on conventional equipment) is assumed to be 400 bar, whereas that of the smaller particles with UHPLC equipment is assumed to be 1200 bar. For separations requiring up to about 100,000 plates, the curve for the 1.8 μm column lies well below that of the 3.5 μm column, showing that a faster analysis can be achieved. Only for the relatively unusual case of the requirement of >100,000 plates does the excessive pressure of the increasing long column required prevent the profitable use of the smaller particle column.

While the original particle size of the new generation shell column was of the order of 2.5 μm, columns packed with sub 2μm shell particles are now widely commercially available and can give further improvements in performance, if appropriate instrumentation is available[31,32]. This improvement can be seen for the kinetic plots in Fig. 3 (b) where separations requiring around 20,000 plates can be achieved in around 1 minute on a 1.6 μm shell column, but require significantly longer on the totally porous column of about the same particle size (1.8 μm).

The possible advantages of core shell materials with considerably smaller particles (1.0-1.3 μm) has been investigated, including a commercially available 1.3 μm material having a 0.9 μm non-porous core and a porous shell < 0.2 μm thick [33-35]. Exceptionally low observed minimum plate heights of 2.2 μm were reported corresponding to a plate count of 450,000 plates/m. However, only short columns of 3-7.5 cm length operated at modest flow rates could be used. Clearly, practical column dimensions and operation are severely limited by the maximum pressure of current instruments, and their band spreading effects. Only the lowest extra-column bandspreading instruments could be used to obtain these results. Nevertheless, it was observed that the extra-column bandspreading could have a major impact on the apparent kinetic performance; significant plate count loss was noticed for retention factors <5, even with the best system that was used for the experiments, which had $\sigma^2_{(extracolumn)} = 2\ \mu L^2$ at the flow rates used. It was also demonstrated that the loss in performance caused by frictional heating effects remained negligible, but the short column lengths and flow rates used must clearly be taken into account when considering this observation.

The performance of 1.3 μm particles was further studied in the gradient elution mode[36,37] with both small molecules and peptides (which have different diffusion characteristics). The material appeared to be particularly well-suited for fast separations, but the advantages were much more obvious for peptides than small molecules. This was due to the possibility of working closer to the optimum flow velocity for peptides, as they have smaller mobile phase diffusion coefficients . Kirkland[38] debated whether sub 2 μm shell particles were really necessary in many practical applications. While the introduction of shell particles in the sub- 2μm range as opposed to the original 2.5 -2.7 μm particles allowed very fast separation, the efficiency advantages of these very small particles may often not be realised nor sufficient to overcome some of the practical limitations and disadvantages of their use. A 2.0 μm particle diameter was suggested to retain many of the advantages of these particles, while minimising some of their disadvantages.

The advantages of shell columns can be extended to their substitution for conventional larger particle 5μm totally porous phases[39]. The large size core-shell particle columns show a clear improvement in separation power over their fully porous counterparts by allowing faster separations (at the same efficiency) or a higher separation resolution (at the same analysis time). Van Deemter and kinetic plots showed that superficially porous particles of 5 μm diameter provide a superior kinetic performance compared with the fully porous particles over the entire range of separation conditions, when both types of support were evaluated at the same operating pressure. The same observations were made both for isocratic and gradient analysis[40]. It was demonstrated that the shell particles do not compromise sensitivity due to loadability issues, and that these columns could be used on conventional equipment without modification to obtain significant improvement in analysis time, especially if columns of 4.6 mm ID packed with larger particle size (~2.5 μm) are utilised, which reduce the need for instrumentation giving a low extracolumn bandspreading contribution [41-43]. Gritti and Guichon[44] found values of the minimum reduced plate height of 1.3-1.5 for shell columns of 4.6x 150 mm packed with 4.6 μm shell particles. The separation speed and resolution of these columns was claimed to be equivalent to that of 2.5 μm totally porous particles for hold up times larger than only 10s, and virtually equivalent to that of 2nd generation silica monoliths. The latter were stated to have the disadvantage that they can only be used at pressures up to 200 bar.

Care must be taken when comparing the performance of packings in columns of different physical dimensions, as particularly the internal diameter of the column can influence the performance[41-44] (see below). The minimum reduced plate height of shell columns packed with 4.6 to 1.3 μm particles in narrow bore (2.1 mm) ID format was 1.6-1.9 , which is somewhat higher than the values achieved in the larger 4.6 mm format (see below).

2.3.2 Reasons for the high efficiency of shell particles.

Tallarek[45] conducted a computational investigation of longitudinal diffusion, eddy dispersion and trans-particle mass-transfer in bulk random packings of core shell particles with varied shell

thickness and shell diffusion coefficient. An excellent summary of current knowledge of the various band spreading processes within a column was given. The van Deemter equation gives a simple description of these processes:

$H = A + B/u_{av} + Cu_{av}$

The B term is related to an apparent, complex diffusion coefficient accounting for the sample diffusivity in the interparticle bulk eluent and in the pore network of the stationary phase.
The C term (mass transfer term) accounts for all mechanisms resulting in a finite response time for transfer between solid and the bulk liquid mobile phase.
The A term includes contributions to flow biases taking place over different characteristic lengths in the column that can be divided into:

(i) transchannel (associated with the dimensions of the interparticle channels between neighbouring particles)
(ii) short-range interchannel (associated with the scale of a few particle diameters)
(iii) long range interchannel (associated with the distances between local defects in a packing)
(iv) transcolumn effects (associated with heterogeneities at the scale of the column dimensions).

It was pointed out that the coefficients in the equation are semi-empirical and as a consequence cannot be directly related to a physical description of the individual mechanisms.
Gritti and Guiochon[46,47] had previously outlined these various processes, and proposed that the good performance of shell columns resulted from a smaller B term (due to the non-porosity of the core giving a reduced packed bed volume accessible for diffusion) and a much reduced A term. Other work indicated that the smaller A term in shell columns was mainly due to a higher transcolumn homogeneity rather than an improved bed morphology on smaller length scales[48,49].
It was shown that when analysis of small molecules was performed at (for isocratic) or somewhat above (for gradients) the optimum flow, the eddy diffusion term contributes the great majority of the band broadening. The greatest contribution to eddy dispersion is from wall and/or border layer trans column effects. As the bed aspect ratio (the ratio of the column to particle diameter)

increases, the column performance tends towards the infinite diameter column[50]. A study which compared the performance of columns packed with 100 x 2.1, 3.0, 4.6mm fully porous RP BEH particles showed a systematic decrease in efficiency for uracil (an unretained compound) at high flow velocities with decreasing column ID. This is due to the increasing volume fraction of the wall region. Here, at a distance of up to 5 particle diameters from the wall, the average linear velocity of the mobile phase is about 10% larger than in the central region. For retained compounds, the effect is smaller as the difference is levelled out due to the longer residence time of the compound in the column. The computational study[45] concluded that for bulk random packings (for which A terms iii and iv are not applicable), the improved performance of shell columns is mainly due to reduced trans-particle mass transfer resistance and transchannel eddy dispersion.

Due to their complex mode of preparation, the reproducibility of the manufacture of shell columns might be questioned especially with regard to the reproducibility of the eddy diffusion and its effect on the total efficiency. However, studies have indicated that for several different commercially available products, reproducibility was good. Differences in column efficiency between columns were attributed merely to the random nature of the packing process and the resulting lack of homogeneity of the column bed[51]. For 2.6 μm commercially available shell particles in 2.1 x 100mm column formats, the rsd of the eddy diffusion contribution was less than 10% [52]. Similar results were found for shell particles with larger pore size designed for the separation of peptides[53] .

The question of the monodispersivity of the support and its influence on column performance has long been a subject of debate amongst researchers in this area. Shell particles have a very narrow particle size distribution (rsd ~ 5%) and it seems possible that this could indeed influence the A term in some way. It should also be considered that practical reasons and perhaps greater ease of packing particles of narrow psd may be important. Felinger developed a theoretical framework for calculation of the effect of psd on efficiency, demonstrating that a wider psd was detrimental to performance[54]. A constant packing density was assumed in this work. Psd mostly affects intraparticle diffusion, therefore its effect is negligible in the case of small molecules. However,

its influence increases as the size of solute molecules increases, because intraparticle diffusion becomes increasingly significant. Thus shell particles with a narrow psd should be advantageous. It was shown that bimodal phases (which consist of deliberate mixtures of particles of different size) had no advantage over unimodal phases-manufacturers are known to sometimes add small quantities of larger particles to a UHPLC packing in order to reduce the operating pressure.

Recently, narrow psd fully porous packings have become available, and their properties have been briefly reviewed[15]. By comparison of their performance with shell columns, some elucidation of the factors leading to high efficiency might be possible. Guiochon and co-workers [5556] studied 2.1 and 3.0 mm ID column packed with such materials (Titan C18) of nominal particle size 1.9 μm. These materials had particle size distribution of rsd 10 % , intermediate between that of classical porous particles (~20 %) and shell particles (~5 %). The Titan material exhibited low reduced plate height (h) values of 1.7-1.9, which is low for totally porous particle columns although does not reach the even lower values exhibited by some shell columns. The authors pointed out that it was tempting to therefore assume a correlation between narrow psd and high efficiency. However, they attributed the performance instead to the unusually small diffusivity of analytes across the Titan porous particles (about a factor of 3 lower than for typical porous C18 particles), leading to the lowest h values being obtained at low reduced velocities (around 5 instead of 10). Therefore the performance is attributable to a reduction in the B term. An undesirable consequence however, is a larger C term, which leads to poorer performance at high mobile phase velocity. Increasing the pore size of the material from 80-120Å produced improvements in the efficiency of the columns when applied to the analysis of peptides and small proteins[57,58].

2.3.3 Effect of shell thickness, and of pore size, on performance for small and large molecules. Effect on loading capacity.

The effect of shell thickness has been studied particularly with regard to the separation of large molecules. In general, studies have suggested a compromise between a short diffusion path (which leads to high efficiency) and adequate retention / mass load tolerance. Shell particles with thinner porous shells show marginal improvement in column efficiency for small molecules, but

improved performance for larger molecules which have much smaller diffusion coefficients and thus give higher mass transfer contributions to band broadening[59]. This particular study indicated the best compromise for large molecules was a 0.2 μm shell thickness. This value represents a rather thinner shell than used in the original materials[11] which reflects the slower diffusion of large molecules and its consequent negative influence on mass transfer.

For the separation of larger molecules such as peptides and proteins[60] the pore size must be large enough to accommodate the solutes; wide pore materials are now commercially available [61]. Wagner et al estimated that solutes with MW >5000 could show restricted diffusion and poor performance in 2.7 μm shell packings with a conventional pore size (e.g. 90 Å) while packings with pore size 160 Å were limited to solutes of MW <15000. 400 Å materials were suitable for proteins with MW 400 kDa or higher[62]. Further work explored in more detail the added effect of shell thickness on performance using particles of diameter 3.4 μm with different pore size over the range 90-400 Å and shell thickness 0.15 - 0.5 μm for the separation of proteins[63]. Work with the larger pore size material 400 Å with appropriate surface area confirmed that large molecules (even up to 500 kDa) have unrestricted access to the bonded phase of the material. Other studies[20] have compared the performance of 2.7 and 3.5 μm particles with shell thickness 0.1-0.5 μm and pore size either 300 or 450 Å prepared by the coacervation procedure and functionalised with C18 or C4 ligands. In this recent study, little difference was found in isocratic (H or h) or gradient performance (peak capacity) for 2.7 μm particles with either 0.52 or 0.23 μm shell thickness when tested with carbonic anhydrase (MW 30 kDa). Using the same solute, much improved (about half the) plate height was obtained on 2.7 μm particles with 450 rather than 300 Å pores. Furthermore, whereas for small molecules, d_p has an important effect on performance (N is approximately inversely proportional to d_p), the performance for carbonic anhydrase was almost the same on the 2.7 and 3.5 μm columns.

Glennon and co-workers[64] studied the preparation of shell particles of overall diameter 1.5, 1.7

and 1.9 μm coated with a thin 50 nm shell. The materials were comprehensively characterised using scanning and transmission electron microscopy, dynamic light scattering, gas adsorption (BET), elemental and thermogravimetric analysis, diffuse reflectance FT-IR (DRIFT) and inverse size exclusion chromatography. The minimum reduced plate heights were around 4; this value was larger than that for a 1.7 μm packing with a thicker 150 nm shell.

While much work has centred on the question of the pore size of shell particles, it seems that the pore size distribution of these materials is considerably wider than that of totally porous packings, as demonstrated using inverse size exclusion chromatography[65]. This observation is perhaps unsurprising in view of the completely different methods used to produce these different kinds of particles, and must arise from the method of shell synthesis.

The loading capacity of shell particles is sometimes questioned in that only a proportion of the particle is porous and therefore accessible to solutes. The capacity of shell particles was found to be not greatly reduced compared with totally porous particles yielding similar efficiency[12,66]. The original small particle shell columns[11] had a value of ρ of 0.63, indicating that about 75 % of the particle is porous compared with a totally porous particle of the same particle diameter. Other popular commercial varieties of shell column have a solid core of diameter 1.9 μm and an overall diameter 2.6 μm, implying a value of $\rho = 0.73$ and around 61 % of porous volume. The ρ value of close to 1 for the original pellicular particles indicates a very much smaller porous volume. In view of these values, there is no particular reason to suspect that for these small "thick" shell particles that the loading capacity should be drastically compromised, although clearly their capacity might be expected to to be somewhat reduced. However, this favorable assessment may not be true for more recently developed shell packings with different shell thickness. In addition, other factors may be involved in loading capacity; it is possible that solutes do not penetrate completely to the centre of totally porous particles, indicating that some of their potential capacity could be redundant. Furthermore, the specific surface area of the porous shell (in m^2/g of shell material) may be different from that in totally porous particles.

The fundamental cause of overloading in the porous fraction of shell particles or in totally porous particles on RP materials has been the subject of much debate. Small neutral polar molecules like phenol and caffeine have been proposed to experience weak adsorption sites at the interface between the solvated C18 bonded layer and the bulk eluent, while high energy sites are intercalated deeper within the grafted C18 chains[67]. For charged compounds, the high energy adsorption sites are scarce while their binding constant on the abundant weak adsorption energy sites is low. Recent work confirms the existence of three distinct pore regions at increasing distance from the surface: solvated C18 layer, interface, bulk mobile phase. Hence, there is the possible co-existence of distinct adsorption sites which are scarce at the silica surface, with some existing amidst the solvated C18 chains with most in the interface region. Ionised solutes, which typically show much greater tendency to overload because such solutes must reside inside a small portion of the interface region at a specific distance from the pore wall. Here, the hydrophobic moieties can favourably interact with the C18/acetonitrile mixture closer to the pore wall, while the charged head remains solvated by the water rich bulk eluent at greater distance from the wall[67].

2.3.4 Small particles in capillary column format.

Much of the driving force for the use of capillary columns in HPLC has come from the positive influence of their low flows on detection methods such as UV and mass spectrometry. For the same volume of solution of the same concentration, concentration-sensitive detectors such as UV will show increased response for very narrow-bore columns, as the same solute mass is presented to the detector in a smaller volume of mobile phase. Nevertheless, the advantage is limited to situations where the volume of the sample is restricted, as narrow-bore columns are easily overloaded in mass or volume terms, whereas the capacity of larger columns is increased in proportion to their increased volume. The situation in electrospray mass spectrometry is different. An electrically charged droplet spray is generated in the presence of a strong electric field. Solvent evaporates and solutes become ionised. Lower flow rates produce smaller droplets that have a higher surface to volume ratio, enhancing desolvation and ionisation efficiency and leading to an increase in sensitivity. Nevertheless, modern ion sources incorporate measures to

limit sensitivity losses at elevated flow rates, and mass spectrometry under some circumstances may behave in a mass-sensitive way, with little influence of flow rate or column bore on sensitivity[68]. It remains to be seen what impact the latest developments in MS interface technology will have on the use of capillary columns. Nevertheless, capillary columns retain other advantages such as considerably reduced effects of frictional heating, and possible enhancements in performance due to slip flow (see below).

Tallarek and Jorgenson[69] investigated the effects of slurry packing concentration using totally porous bridged ethyl hybrid particles of 0.9, 1.7 and 1.9 μm diameter, and of 1.9 μm shell particles on the efficiency of capillary columns of 30-70 μm i.d. having an aspect ratio d_c/d_p > 25. Using higher slurry concentrations (20-100 mg/mL) gave higher efficiency columns than low concentrations (2-3mg/mL). Confocal laser scanning microscopy showed that higher concentrations suppress particle size segregation but at the expense of producing packing voids. Only a few voids were found with shell particles; nevertheless, their efficiency was found to be lower than with the fully porous particles. Different results concerning slurry concentration were obtained with smaller i.d capillaries. Performance was impressive for these larger diameter capillaries, which showed h_{min} as low as 1.6, although even better performance was obtained with the narrower i.d column (h_{min} as low as 1.2)[48]. The authors stated that more work was necessary to rationalise these results and extend the finding to interpreting the performance of conventional diameter columns.

Jorgenson further evaluated the properties of 1.1 μm shell particles having 187 Å pore size that were packed into 30 μm ID capillaries, using electrochemical detection[70]. The particles were synthesised from colloidal silica and bonded with octadecyldimethylchlorosilane. The minimum reduced plate height obtained was 2.6. It was considered that the psd of the stationary phase might influence the packing process, as size segregation may occur across the column diameter, which increases the eddy diffusion term in the van Deemter equation. Conditions for slurry packing of the capillary were also studied; a methanol slurry with a slurry concentration of 2.5% was found to give optimum efficiency.

Some practical investigations of the performance of packed capillaries have been published. For instance, Novakova investigated the performance of 75 μm i.d capillaries packed with 2, 3 and 5 μm fully porous particles for the separation of peptides resulting from the tryptic digest of various proteins[71]. Pressures of up to 800 bar were utilised. Peak capacities up to 500 could be obtained using a 120 minute gradient using a 2 μm column. A temperature of 60 ^{o}C was used to enhance solute diffusion and to reduce mobile phase viscosity.

The performance in gradient elution using kinetic plots was compared for capillaries packed with fully porous 3 and 2.7 μm core-shell particles, and for a capillary monolith. A tryptic digest of bovine cytochrome c was used as an evaluation sample. Despite the presence of the solid core, the gradient performance of the superficially porous particles was found equal to that of the fully porous column. The monolith showed the least contribution to mass transfer and its permeability was higher than for the packed columns. Hence the monolith showed the best performance for both fast and for high capacity gradient separations[72].

Wirth has investigated the possibilities of slip flow using sub- micron particles, especially as applied to the analysis of proteins[73-76] with capillary columns of small inner diameter (e.g. 75 μm). In theory, the velocity of the mobile phase at the column wall is zero according to Hagen-Poisuille theory, but this is only true if the attractive interactions between the mobile and stationary phase molecules is exactly the same as that between the mobile phase molecules themselves. This is far from true in reversed-phase (RP) separations because attraction between the hydrophobic stationary phase and the mobile phase molecules is small. Consequently, the velocity at the wall is non-zero. As a result, the backpressure of these columns was much lower than expected, and the reduced plate height was also much lower, with a value of 0.032 observed. Indeed, in the presence of slip flow, the mobile phase velocity distribution in the column should be reduced, resulting in a smaller plate height. Yan and Wang[77] considered that the specific contributions of the ordered packing, the slip flow effects, and the solute molecular size to this

result were unclear. Using numerical methods, they predicted the smallest value of h in the absence of slip flow was 0.084, a value of h closer to that found by Wirth, who had used a higher value (h = 1.0) predicted from a previous investigation by Schure[78] for a face-centred cubic crystalline structure, which is adopted by this type of column packing . Thus they believed that some of the efficiency advantage claimed to be due to slip flow had been incorrectly attributed. They calculated that the smallest value of h in the presence of slip flow under similar experimental conditions was 0.059, which remains larger than the value of 0.032 claimed by Wirth. They believed that the difference could be explained in that their calculation had not taken into account the large molecular size of proteins, which may be excluded due to their size, from regions of stagnant flow. Thus they considered that the small value measured by Wirth was not unexpected. They recommended that further studies should be carried out with small molecules to further elucidate the contribution of the various effects.

Wirth[79] and co-workers welcomed this new theoretical investigation. They distinguished between slip flow in open capillaries, which are a much more well-defined system compared with the usual approach of utilising packed beds in LC. They showed [75] that the flow enhancement caused by slip flow greatly increased as the diameter of particles coated with a mixed monolayer of C4 and C1 decreased from 1300 nm to 125 nm . They agreed also with the hypothesis that proteins could show a reduction in h below that expected from theory because they could be excluded from stagnant regions nearer to the surface of particles. It seemed that improved efficiency could be obtained when the analyte radius is significant relative to the particle diameter. For the case of the protein bovine serum albumen, this ratio is 1.5 %. They concluded with agreement with the results of Yan and Wang[77] that extraordinary values of h are possible even without slip flow, that flow rate is enhanced by slip flow and that use of particle diameters tailored to the analyte diameter might give a lower h by excluding analyte from stagnant regions.

Desmet and co-workers[80] also compared plate height for slip and non-slip conditions, this time using direct numerical simulation which solves the original problem by transiently monitoring mass transfer in the system. This technique is more computationally intensive but simulates the real physical behaviour of band broadening. Their results suggested that the impact of slip flow

on chromatographic performance was minimal, because it can only partly reduce the mobile phase band broadening contribution (by about 40-70 %), and because this type of band broadening is only a fraction of the total plate height. Slip flow affects the mass transfer contribution. Desmet estimated a much higher minimum reduced plate height than the value of 0.032 reported by Wirth and co-workers. It was proposed that the performance gain shown by Wirth could be linked to the use of non-porous particles, which have no stationary phase band broadening contribution. They considered their results similar in nature to those of Yan and Wang.

Non-porous particles are advantageous when applied to the separation of proteins. It was argued that whereas a 100 kDa protein has a diameter of about 100 Å, it will not diffuse readily even into the 300 Å pores of many conventional porous chromatographic materials designed for this application; it will access less than 50 % of the pores[81]. A 1200 Å material is necessary for such a solute to access 90% of the pores. An alternative approach is to use non porous particles of 0.5 μm diameter. It seems that the greatest advantage of slip flow with 0.5 μm particles is with large molecules. For small molecules, the C term (mass transfer term) in the van Deemter equation is very small anyway, so the improvement in performance is much less. Wirth has recently summarised work on slip flow and submicrometer particles[82]. The methodology was again recommended particularly in the separation of intact proteins[83 84]. In the form of monoclonal antibodies, protein- based drugs represent the fastest growing segment of the pharmaceutical industry. Wirth further pointed out that their experiments had mostly employed techniques that avoided the contributions of instrumental band broadening. For instance, capillaries were dipped into protein solutions to accomplish injection, and on-column detection was performed by fluorescence imaging. However, transferring the column methodology to a commercial nano-LCMS system produced peaks which were approximately an order of magnitude broader. Clearly, there are some difficulties that must be overcome in the more general practical implementation of this work.

3 Frictional heating effects.

The detrimental effects of frictional heating caused by percolation of the mobile phase through a packed bed, have been considered since the early days of HPLC. The power P generated in watts within the column is given by

$$\text{Power} = \Delta P \times F$$

where ΔP is the pressure drop(in SI units N/m^2) and F is the volumetric flow rate (m^3/s) through the column[85,86]. The heating effect produced can give rise to both axial and radial temperatures gradients in the column. Axial temperature gradients are formed with temperature generally increasing further down the column length. These can lead to changes in solute retention; in reversed-phase separations, a decrease in solute retention is usually observed. Radial temperature gradients are caused by loss of heat through the column walls causing the centre of the column to be at higher temperature than the wall region. Thus, a spread of velocities across the column radius occurs, that can lead to serious band broadening. Usually, the column is maintained in as adiabatic an environment as possible, to restrict heat losses and minimise the radial temperature gradient, although such an approach tends to maximise the axial gradient.

It has been known for some time that band broadening effects are lower in columns packed with shell particles, thought to be due mainly to the relatively high thermal conductivity of the solid silica core[87]. Jorgenson also observed enhanced heat dissipation in columns of 1.6 μm shell particles compared with fully porous 1.8 μm particle columns. A water jacket was used to enclose the column, and compared with the performance of the standard column oven (Waters Acquity), the former providing conditions remote from the adiabatic approach and that should maximise the effects of radial temperature gradients[88]. Measurements of temperature with a micro thermocouple situated adjacent to the column outlet frit indicated hardly any increase in temperature for the shell column and van Deemter curves of reduced plate height against reduced velocity showed little upturn of the plots for this column, even when used in the water bath. In contrast, the totally porous column showed marked upturn in the plots at higher velocity when situated in the water bath. Nevertheless, it is possible that even the shell column could have

shown reduced performance if higher reduced velocities than used in this study had been employed.

4. Effect of pressure on retention; combined effect of frictional heating and pressure on retention.

The influence of pressure alone can be studied by adding narrow bore restriction capillaries to the end of the column. Such experiments also allow the calculation of the change in partial molar volume ΔV of the solute associated with its transition between the mobile and stationary phase.

$\Delta V = V_{stationary} - V_{mobile}$

Alternatively, it is possible that changes in the volume of all of the components in the system should be considered. Thus it may represent the volume change of the system between the "solute bound to the stationary phase" and the "solute in the mobile phase". Changes in ΔV are greater for large molecules such as peptides and proteins[89]. A study including a number of different polymeric and monomeric bonded RP materials indicated that difference in molecular size was the most important factor governing increases in retention with pressure, even when considering smaller molecules[90]. Binding of large molecules may thus result in the greater volume reduction of the system including the solute, stationary phase and mobile phase. It is possible that large molecules may be more compressible in the stationary phase than small molecules, or that these results may be connected with the greater area of contact between large molecules and the stationary phase and changes in solvation. A C30 column gave interesting selectivity changes between planar and non-planar solutes as a function of pressure. Polymeric C18 and C30 phases were further shown to be useful for the separation of isomers of C18 fatty acids and tocopherols, especially at high pressure [91]. Changes in the particle size of a given type of stationary phase (for example, changing from an HPLC to a UHPLC phase) can cause changes in selectivity due to the different effect of pressure on solutes of different types. Changing the flow rate on a given column results in changes in pressure and in retention caused by temperature changes. In RP the effect of increased pressure tends to give increased retention, which opposes the effect of higher temperatures which reduce retention. Alternatively in hydrophilic interaction

chromatography, both increased pressure and increased temperature caused by increased flow act in the same direction to reduce retention[92]. The combined effect of pressure and friction-induced heating on the retention of small molecules and proteins has been studied[93 94]. For large molecules, the impact of pressure seems to overcome the effect of frictional heating, although the temperature effect was not negligible. The interpretation of the results was however, complicated by possible changes in the structure of the proteins with elevated temperature and pressure, effects which are protein dependent. For proteins, the effect of increasing pressure (which tends to increase retention in RP-LC, especially in the absence of frictional heating which tends to reduce retention) can even be seen in gradient elution. This is unusual, because changes in retention with increase in mobile phase elution strength are generally large compared with other effects, especially for large molecules. The successful deconvolution of the temperature and pressure effects in this work required two experimental systems[93,94]:

a) the combined effect of pressure and mobile phase velocity (frictional heating) is monitored (variable inlet pressure mode) by varying the flow rate from 0.1 mL/min up to that which generates a pressure drop of 750 bar over the column.

b) the effect of mobile phase flow velocity alone was monitored by systematically decreasing the flow rate while maintaining the pressure drop constant at 750 bar (constant inlet pressure mode).

5. New support formats.

Pillar array columns were first proposed in 1998 for use under electrically driven flow conditions[95]. A pillar array can be considered as the 2-dimensional equivalent of the sphere packing in a packed bed. It is produced by micro-machining in silicon or glass, and has the advantage that the pillars can be arranged in a perfectly ordered and reproducible array, offering a dramatic reduction in eddy dispersion. Long columns (3m) with optimal pillar diameters (5 μm) and interpillar distance (2.5 μm) could produce 1 million theoretical plates when using a pressure restricted to 350 bar[3]. Desmet and co-workers [96] provided experimental and theoretical proof that a microfabricated packed bed column uniformly filled with radially elongated pillars (REPs, see Figure 4), can produce the same separation performance as open-tubular columns, which are

often regarded as the optimum possible column format. A monolayer of octylsilane can be coated on the external surface of the pillars. In REP columns the pillars have a radially elongated, diamond shape as opposed to cylindrical shape, which is the 2D equivalent of spheres. The REP variant of pillar columns has been shown to lead to a significant reduction in the minimum plate height[97,98] . It was shown that as long as pressure is not a limiting factor, these REP columns could even outperform the open-tubular format with significant gains in either speed or efficiency that are proportional to the tortuosity of the bed. With these columns of length 4cm, it was possible to achieve 160,000 theoretical plates for unretained analytes and 70,000 plates for retained analytes, despite the relatively large interpillar distance (2.5 μm). Song et al[99,100] reported the fast quantitative analysis of branched chain amino acids using pillar arrays manufactured on microchips using multi-step UV photolithography and deep reactive ion etching. The pillar array was functionalised by treatment with dimethyloctadecylsilane. The method was used for the analysis of sports drinks and human plasma samples and showed good agreement with the results of conventional HPLC procedures.

6 . Monolithic silica columns.

6.1 General Considerations.

Monolithic silica columns, developed in the 1990s and commercialized in 2000, seemed to be able to provide the performance exceeding the limit of performance of a column packed with totally porous particles on the basis of a large (through-pore size) / (skeleton size) ratio of 1-2, (compared to 0.25-0.4 for a particulate column)[7]. The first commercialized monolithic silica column clad with PEEK, Chromolith Performance RP-18e (4.6 mmID, 10 cm), possessing through-pore size of ca. 2 μm, skeleton size of ca. 1.3 μm, external porosity of 0.65 and total porosity of 0.75, could provide ca. 10,000 theoretical plates, or a height equivalent to a theoretical plate (HETP) H=8-10 μm at an optimum (mobile phase linear velocity, u=1.5-3 mm/s), with high permeability ($K=6x10^{-14}$ m^2)[2]. The column efficiency was equivalent to that of a column packed with 3.5-4 μm particles with pressure drop (or permeability) equivalent to a

column packed with 7-8 μm particles, the total performance (efficiency and pressure combined) seemingly leading the field [101].

Monolithic silica capillary columns in early times were prepared in 50-200 μm ID fused silica tubes from tetramethoxysilane (TMOS) or a mixture of TMOS and methyltrimethoxysilane (MTMS) to possess external porosity greater than 80% and total porosity as much as 96%[102]. The capillary columns afforded H=8 μm at optimum (u=0.5-1.5 mm/s), with permeability $K=8x10^{-14}$ m^2. The HETP and K values corresponded to those of a particulate column packed with 4 μm and 8-10 μm particles, respectively. Larger sized 0.53 mm ID silica monolith capillary columns prepared from the mixed silanes could generate H=11-13 μm with similar permeability ($K=5.2\text{-}8.4x10^{-14}$ m^2)[103].

Preparation methods and fundamental properties of monolithic silica columns were summarized in previous reviews[104,105]. Alkoxysilanes such as TMOS or tetraethoxysilane (TEOS) undergo hydrolytic polymerization accompanied by phase separation in aqueous acetic acid in the presence of polyethylene glycol (PEG) to form monolithic silica having bicontinuous network structures[106]. The amount of PEG in the feed controls phase separation during polymerization[107]. Mesopores were formed subsequently by treating the monolith with aqueous ammonia solution. The structural characteristics of the silica monolith including high external porosity, and large through-pore size and skeleton size were the sources of relatively low efficiency by today's standards.

6.2 Advances in monolithic silica columns for reversed-phase LC.

6.2.1 Improvements proposed based on the characterization of first generation materials.

Desmet et al. pointed out, based on the kinetic plot analysis of first generation monolithic silica columns (rod and capillary) possessing ca. 2-8 μm through-pores and 1-2 μm skeletons, that the through-pores and skeletons of the first generation monolithic columns were too large and the

external porosity too high. In other words, they suggested to compromise the major characteristics of monolithic silica for higher column efficiency[108]. The presence of through-pores of ca. 2 μm is shown to cause a large mobile-phase mass transfer contribution to band broadening. Characterization of silica monoliths has been subsequently carried out using inverse SEC as well as microscopic methods, SEM, TEM, and confocal laser scanning microscopy (CLSM), in addition to mercury porosimetry and gas adsorption.

Guiochon et al. found heterogeneity in the network structure from the center to the wall region on first generation Chromolith by placing a detection point at different radial positions[109]. Tallarek et al. studied the monolith with CLSM to reconstruct the structure to find heterogeneity in first generation monolithic silica[110]. Central point injection of samples and curtain flow elution with Chromolith showed improved efficiency by a factor of two or more, indicating the existence of some heterogeneity in the wall region of monolithic columns and higher homogeneity of the central region[111].

In order to maintain the advantages of the monolithic structure, the large (through-pore size)/(skeleton size) ratio must be retained, the external porosity and through-pore size must be reduced, and the higher external porosity compared with that of particulate columns should be maintained. This in turn required much reduction in the skeleton size for improved efficiency. Desmet also predicted that improved performance for high-speed separations (small N) would be possible with the increase in phase ratio or the amount of skeletons relative to the through-pores[112]. Actually, the approach is somewhat similar to the reduction in particle size in a particulate column. An important difference from the case of particulate column is that a change in external porosity is possible, especially at higher values than for a particulate column.

6.2.2 Preparation of second generation monolithic silica columns.

Hara successfully improved the column efficiency of silica monolith in a capillary by increasing the silane content relative to the aqueous portion in the preparation feed to reduce the porosity or

to increase the phase ratio, and increasing the PEG content to retard phase separation, in turn to reduce the domain size[113]. The changes in preparation conditions resulted in reduction in external porosity to 0.65-0.76 and in the domain size (skeleton size + through-pore size), an increase in phase ratio, and most importantly, increased homogeneity compared to first generation monoliths in capillaries. The column with the smallest domain size, 1.3 μm through-pores and 0.9 μm skeletons provided the highest efficiency, H=ca. 5 μm (similar to 2-2.5 μm particles) at u=ca. 3 mm/s with $K=4.7x10^{-14}$ m^2 (similar to a column with 5 μm particles showing very high permeability). Higher efficiency and higher permeability were observed compared with those of some first generation columns, indicating the increased homogeneity of the second generation materials.

Nakanishi and coworkers prepared silica monoliths using TEOS and nitric acid in the presence of poly(acrylic acid) (PAA) instead of TMOS, acetic acid, and PEG, and clad the silica rod with silicate glass[114]. The glass-clad silica rod, 2.4 mmID, 9 cm, produced H= 6.9 μm. It was shown that another combination of silane, acid, and polymeric surfactant in the feed was able to afford high-efficiency silica monolith.

The mesopore structure was also improved. Hara et al. reported the effect of hydrothermal treatment on pore properties and column efficiency of silica monolith in capillaries prepared from a mixture of TMOS and MTMS[115]. The effect was observed in improved column efficiency for peptides depending on solute size, although it did not appreciably affect the efficiency for alkylbenzenes with minimum plate height, H=4-6 μm observed at u=ca. 2 mm/s.

Cabrera reported second generation silica monoliths clad with PEEK resin, commercially available as Chromolith HR that showed similar improvement[116]. The second generation product possessed 1.1-1.2 μm through-pores and sub-micron skeletons with external porosity of ca. 0.6 to produce H=5.5 μm (equivalent to a 2-2.5 μm particle column), and K=ca. $2.4x10^{-14}$ m^2,

(equivalent to 3.5 μm particles). The pressure required for the same flow rate is about 2.5 times higher than for first generation Chromolith, while the column efficiency was more than 50% greater.

6.2.3 Characterization of second generation monolithic silica columns.

Second generation monolithic silica columns were characterized by several groups. Chromolith HR and the first generation product Chromolith Performance were examined by inverse size exclusion chromatography by Felinger et al[117]. Smaller through-pores by 40%, and increased mesopore volume by 30% indicating an increase in phase ratio, were reported. Central point injection of samples and curtain flow elution with second generation Chromolith showed improved efficiency by up to 50%, a smaller increase compared to first generation column, indicating higher homogeneity of the second generation monolith[118].

Gritti and Guiochon examined two types of second generation monolithic columns by determining eddy diffusion term in band broadening[119,120]. They attributed the increased column efficiency, H=5-6 μm for one type of monolith and 6-7 μm for the other, to increased radial homogeneity in the network structure of the second generation monoliths, in addition to reduction of the domain size. They also pointed out that the monoliths still showed some radial heterogeneity.

Tallarek and coworkers examined the second generation monoliths with chromatographic methods, mercury intrusion porosimetry, SEM, and CLSM. Figure 5 shows a three dimensional reconstruction of a silica monolith with 0.81 μm through-pores based on CLSM. They found smaller through-pore and skeleton size than in first generation silica monoliths, and concluded that the monolith structure possessed high radial homogeneity except for a small region at the wall, and also high homogeneity of the bulk region[110,121]. The study on correlation between morphology and column efficiency led them to suggest the contribution of column end structures to the column efficiency, or border effects.

Cabooter and coworkers found that the second generation monolith showed higher efficiency than the first generation materials. However, the second generation monolith structure was associated with much reduction in permeability, hence actual improvement was realized only for separations requiring 45000 theoretical plates or less (Figure 6)[122]. This is very similar to the effect of reduction in particle diameter for particulate columns. They also pointed out that second generation monoliths were still inferior to advanced particulate columns, and if monolithic silica columns were to be really competitive with advanced particulate columns, an increase in structural homogeneity and optimization of external porosity would be required.

Recently comparisons of columns have been described from various points of view. Eeltink and coworkers compared the performance of monolithic silica capillary columns (MonoCap, 0.1 mmID, 5 cm) with those of capillary columns (0.1 mmID, 5 cm) packed with 3 μm totally porous particles or 2.7 μm fused-core particles in gradient elution[123]. At a pressure limit of 350 bar, for both fast and high peak-capacity separations, the monolithic silica column was shown to perform better than the other columns, mainly due to the difference in its permeability. Other studies indicated that core-shell particles provided superior performance to other types in high speed separations, but that high peak capacity separations could be most conveniently carried out with monolithic columns with high permeability using a long column with long analysis times[124,125,126].

Most of these characterization studies on the second generation monoliths indicated an improvement in homogeneity compared to the first generation material, but pointed out that they still possessed inadequate homogeneity in structure and too large a domain size, providing the question as to whether it is possible to achieve further improvements, ie a smaller domain monolith with improved homogeneity.

6.2.4 Development of latest generation monolithic silica columns. Comparison with advanced

particulate columns.

In spite of the difficulty suggested on the basis of characterization of second generation monoliths, improvement in column efficiency has been attempted with monolithic silica columns by reducing the domain size and increasing the homogeneity of the bicontinuous structures. Hara and coworkers studied the effect of PEG on the structure and efficiency of monolithic silica capillary columns with respect to the molecular weight and the concentration in the feed[127]. The silica rod prepared with PEG of higher molecular weight than previous preparations provided submicron domains with high homogeneity, as shown in Figure 7. The capillary column prepared under the optimized conditions showed minimum plate height H=4.1-4.5 μm, at u=2-3 mm/s in comparison with 2.6 μm Kinetex-C18 which showed a similar optimum H, at 4-4.5 mm/s, in a mobile phase of acetonitrile/water(80/20, v/v) at 30 ^{o}C.

The latest versions of the rod columns also showed promising results. Cabrera et al reported prototype Chromolith having sub-micron through-pore size (0.95 μm), and external porosity of 0.57, achieving H = 4.5 μm at 2-4 mm/s, in other words, producing more than 20000 theoretical plates with a 4.6 mmID, 10 cm column, as shown in Figure 8A[128]. Note that the phase ratio was increased considerably from previous materials, as indicated by the smaller porosity. Column efficiency was improved compared to first generation Chromolith Performance by a factor of about 2.

Another series of monolithic silica rod column, MonoTower, prepared from TEOS with nitric acid catalyst, by employing PAA to control phase separation, possessed 0.95 μm through-pores, 0.80 μm skeletons, total porosity of 0.70, and external porosity of 0.55. The glass–clad 2.1 mmID monolithic silica columns encased in a stainless steel tube with epoxy resin filler between the glass and the tube, produced more than 10000 theoretical plates for a 5 cm column (H =4.5 μm at u=2-4 mm/s). The permeability, $K=1.1x10^{-14}$ m^2, was equivalent to that of 3-3.5 μm totally

porous particles[129]. The latest version of monolithic silica columns showed column efficiency corresponding to the performance of sub-2 μm totally porous particles, actually competitive with sub-3 μm core shell particles, as shown in Figure 8B, with ca. 50% less pressure requirement.

A smaller ID monolithic silica column clad with glass, 1 mmID, 5 cm long, afforded similar efficiency as advanced particulate columns of the same dimension with 50% less pressure[130]. Generally lower efficiency, H=ca. 5.5 μm, was observed with 1 mmID, 5 cm columns than that of larger size ID columns even with an instrument providing very small extra-column effects, σ_{extra}^2 < 0.02 μL^2, although the reasons remained unclear, whether it was due to the difficulty in column packing or it originated from the column hardware.

It was also noted that monolithic columns provided higher efficiency than particulate columns for early eluting solutes using the same instrument, and similar or slightly lower efficiency for late eluting solutes (Figure 8C), presumably due to the absence of frits in monolithic silica columns and the presence of larger through-pores causing a greater mobile phase mass transfer contribution to band broadening[129].

It is interesting to note that the two series of monolithic silica columns of the latest generation possessed similar structural parameters and showed very similar performance, in spite of the difference in chemistry of preparation with respect to the silica precursor and the polymer reagent inducing phase separation during gel formation. The results may suggest the possibility of various ways of improvement of the performance of monolithic silica columns. Current issues also include the development of a cladding method to improve the pressure stability, currently 40 MPa with glass-clad monoliths.

The kinetic plots for several columns including monolith and core-shell particles are shown in Figure 8D. They indicate that monolithic silica columns can provide greater maximum number of theoretical plates (N_{max}) than totally porous particles or core-shell particles, but the fast

separation capability has not been proved experimentally yet, although the extrapolation of the plots to the fast separation end may show similar or slightly lower performance than predicted.

6.3 Advantages and disadvantages of rod and capillary columns

Monolithic silica columns are prepared by considerably different procedures for rod-type (conventional size, 1 mm ID or larger) and capillary-type (0.53 mm ID or smaller). The former needs cladding of the silica rod, while the latter prepared in-situ in capillary needs attachment of silica monolith to the tube wall. At present the highest column efficiencies achieved are similar for the two types of monolithic columns at H=ca. 4.5 μm. One feature of monolithic silica columns is that they do not need column packing with particles. This is an advantage, but could also be a disadvantage with respect to preparation of columns of various sizes. It is not so simple as selecting the size of a tube to pack particles. Large through-pores (5 μm) allowing silica nanoparticles (100 nm) to go through can be a feature of monolithic silica of small dimension (4.2 mm diameter, 1.5 mm thick) and conventional size column (3 mm ID, 25 cm)[131].

Preparation and modification of each individual monolith column is of course a disadvantage in terms of reproducibility, and considerable time and intensive labor are needed. Other disadvantages of monolithic silica columns include the problem of homogeneity of modification along the column length, and limitations associated with the reagent in combination with the solvent. Column length is limited in the case of rod columns for the rod prepared to be straight. In contrast very long capillary columns, longer than 200 cm, can be prepared to provide very high efficiency[132].

Monolithic silica capillary columns are associated with some additional limitations as well as advantages. Capillary monoliths of 50-100 μm ID (200 μm ID in rare case) can be prepared from TMOS or a mixture of TMOS and MTMS, but 200 μm ID or larger size columns can be prepared from the mixed silanes only. The larger the capillary diameter, the more difficult is the preparation of the silica monolith, because the silica being formed tends to shrink and comes off

from the wall. Large size monolithic silica capillary columns (0.53 mmID) have not been prepared with efficiency as high as the smaller size capillary columns or rod-type columns. Other disadvantages include the lack of common characterization methods such as gas adsorption and mercury intrusion.

Silica monolithic capillary columns possess advantages including wall-bonded monolithic structure without frits, no requirement of column packing, and most importantly, consistent column efficiency of the monolithic support unless the stationary phase hinders mass transfer of the solutes. Small size monolithic silica capillary columns can be prepared and modified in a meter long tube that could provide a high efficiency HILIC column generating 300000 theoretical plate with a 200 cm column[132]. Monolithic silica capillary columns of good performance can be prepared using information available in the literature and successfully modified while maintaining the column efficiency, as shown in several cited references, for the preparation of reversed-phase [133], HILIC[132, 134, 135, 136], affinity [137], and mixed-mode [138] stationary phases. Successful modification of rod columns was also reported for reversed-phase[139] and chiral stationary phases[128,140,141]. Chemical stability and high temperature stability of the cladding material should be taken into account for rod columns. The availability of monolithic columns as silica encased in thermally stable, chemically inert housing at reasonable cost and column efficiency is desirable.

6.4 New preparation methods and outlook for silica monoliths.

Recently, open tubular capillary columns with a mesoporous silica layer coated to the tube surface were reported. Altmaier prepared silica layers of 0.5 μm thickness on the surface of 10-20 μm fused silica tube, obtaining high column efficiency with very high permeability, 70-450 times greater than for silica monolith capillary columns[142,143]. The columns prepared in a long capillary tube, 3 m in length, generated up to 53000 theoretical plates in normal phase mode, and 167000 theoretical plates in reversed-phase mode with C8 modification. The authors showed separation of a complex pesticide mixture in gradient elution.

Qu and coworkers coated silica nanoparticles (15-30 nm) layer-by-layer on the surface of a 75 μm fused silica tube to obtain open-tubular columns of various coating thickness (0.13-0.60 μm)[144]. The columns (20-50 cm) after ODS modification were able to separate hydrophobic compounds in the reversed-phase mode. The column efficiency was not so high in pressure-driven mode due to the large size of capillary, but up to 54000 theoretical plates were generated by a 20 cm column in CEC mode.

Though it has happened slowly, the gap in column efficiency between monolithic silica and advanced particulate columns has been reduced. Small size columns including capillary columns have been increasingly used with UHPLC, particularly with LC/MS applications. The efficiency of small size monolithic silica columns, 0.1 mmID, 1 mmID, 2.1 mmID, and 3 mmID, is actually reported to be similar to those of sub-3 micron core-shell or sub-2 micron totally porous particles. In spite of the lower pressure limit (for silica rod columns) compared with particulate columns for UHPLC, monolithic silica columns can provide comparable separation speed at lower pressure owing to the higher permeability. In combination with the features of capillary columns, monolithic silica columns may play a role complementary to particulate columns in UHPLC, and possibly a more important role in capillary LC.

The development of small size columns, particularly capillary columns, and that of micro-LC instrument are related to each other. It may depend on how much reduction is necessary in time or in consumption of solvent, or how much increase is required in column efficiency or in pressure with instruments of the next generation. The development of high performance micro-LC instruments as reliable and efficient as current UHPLC or GC instruments is highly desirable.

There were only few papers published on the development and on the characterization of high-efficiency rod-type monolithic silica columns. The principles leading to higher performance are known, yet the improvement does not seem to be prompted by competition. The reasons for

the slow development of improved materials may be due to the technical difficulty or the small number of researchers in this area, or both. One interpretation is the immobilizing influence of strong patents[105]. Modification of silica monoliths in capillaries has been studied by many researchers that may lead to faster development of monolithic silica columns of various types in the future. This has been the case for polymer or organic-silica hybrid monolithic columns consisting of organic and siloxane moieties, as discussed below.

7. Polymer monoliths.

7.1 General considerations.

Among monolithic columns, those based on organic polymers have been studied most extensively two decades after their introduction[145]. Fundamental procedures of preparation, structures, properties, and recent attempts aiming to produce high efficiency for small molecules were included in a review by Svec and Lv[146] covering until late 2014, and in the preceding ones[147,148,149]. This section briefly reviews development of polymer monoliths thereafter with a bias to polymer monolithic columns for high efficiency separations of small molecules in reversed-phase liquid chromatography, including recent development in organic-silica hybrid monolithic columns and examples of high performance gradient separations.

7.2 Performance of polymer monolith columns.

7.1.1 Performance in gradient elution

Polymer monolithic columns can provide high efficiency in gradient elution[148]. Eeltink and coworkers reported the performance of poly(styrene-co-divinylbenzene) monolithic capillary columns for the gradient separation of peptides and proteins[150]. Optimization of feed composition and reaction conditions of the monolith resulted in improvement of performance, the products affording peak capacities of 200 and 100 within ca. 20 and 3 min, respectively, for peptides under ultrahigh pressure conditions (80 MPa), using 0.2 mmID column[151]. Fast gradient separation producing peak capacity of 110 within 210 seconds was shown for a tryptic digest of bovine serum albumin.

Nischang elucidated the performance of poly(styrene-co-divinylbenzene) monolithic column under gradient and isocratic conditions based on gel porosity, and the effect of organic solvent content on solute retention and column efficiency studied by employing solutes of various sizes and various mobile phase compositions[152]. The effect of slow adsorption-desorption kinetics under isocratic conditions that is often associated with polymer gels can be avoided in gradient elution which can provide high efficiency separations approaching to the performance under non-retained conditions, especially with steep gradient and for solutes with high molecular weight, namely peptides and proteins.

The performance of a poly(styrene–co-divinylbenzene) monolith (0.2 mmID, 5 cm) and monolithic silica capillary columns (Chromolith CapRod RP-18e, 0.1 mmID, 5-cm) were compared for the analysis of protein digests by Rozenbrand and van Bennekom[153]. The results showed that the calculated throughput, peak capacity, and identification score were similar for the two columns for single protein digests (BSA or Myoglobin), although the silica monolith provided slightly better results for a more complicated nine-protein digest.

Polymer monolithic columns seem to complement silica-based columns in the high-efficiency separations of high-molecular-weight solutes and biologically active compounds, or when high chemical stability is required. The peak capacity obtainable with a polymer monolithic column of conventional size was shown to be smaller than that with silica core-shell particulate or monolithic column in protein digest analysis[154]. Research on high-efficiency polymer monolithic columns has been carried out in a capillary format in most cases, however, the application of metal-scaffolded columns may enable the preparation and application of conventional-size high-efficiency polymer monolithic columns under high pressure[155].

7.2.2 Performance for small molecules in isocratic mode.

Conventional organic polymer particles and polymer monoliths did not provide column efficiency as high as silica counterparts, particularly in isocratic reversed-phase mode. A decrease

in column efficiency for late eluting solutes, and also at high flow rate, is commonly observed. Suggestions for improvement in performance have included the creation of homogeneous structures of rigid mesoporous skeletons, resulting in considerable surface areas[146,156]. Nischang discussed gel porosity to interpret the properties of polymer supports for LC[157], and suggested that homogeneous network structures of smaller sized skeletons and through-pores with adequate porosity would improve the efficiency for small molecules.

The difference in the state of polymers when they are dry and solvated has been frequently mentioned with respect to polymer support properties. The polymer gel structure in monoliths possessing heterogeneity in the macropores (in micro-scale), and nano-scale heterogeneities due to the distribution of cross-linking density in polymer skeletons, solvated to different extents, have also been suggested as the source of chromatographic properties of polymer monolithic columns[152,157,158]. With the advances in characterization methods including spectroscopic and microscopic methods, more detailed information including those on nano-structures have become available[158, 159 , 160] . They indicated the presence of heterogeneity in polymer monolith nanostructures, in crosslinking density, or in the heterogeneity in three dimensional network structures (in many cases the assemblies of globular structures).

7.2.3 Developments in polymer-based monolithic columns for higher efficiency.

The following are the developments in polymer monolithic columns intended for high-efficiency separations for small molecules under isocratic conditions following those covered by Svec[146]. This has been one of the most active areas in LC research. The approach aims at rigid and homogeneous structures by an increase in crosslinking density, the use of reactive functional groups, and by utilization of living polymerization methods.

Zou and coworkers studied the photoinitiated thiol-yne click reaction of 1,7-octadiyne with 1,6-hexanedithiol or pentaerythritol tetrakis(3-mercaptopropionate) (PTM) [161] , and similar reaction of 1,2,4-trivinylcyclohexane with PTM[162]. A 75 μm i.d. column obtained from the latter

experiment provided permeability, K=3—6x10^{-14} m^2, and plate height optimum, H=10 μm (benzene)—8 μm (BuPh) with *k* = ca. 1-3 at linear velocity, at u=0.7-1.0 mm/s. Interestingly the column gave a smaller H value for more retained solutes in 60% acetonitrile. Evaluation of the column efficiency for a wider range of solutes and in a wider range of mobile phase compositions is desirable.

Lee and coworkers tried to obtain highly crosslinked monolith columns by living radical polymerization of single multi-acrylate/methacrylate-containing monomers (1,12-dodecanediol dimethacrylate, trimethylolpropane trimethacrylate (TRIM) and pentaerythritol tetraacrylate[163]. Column efficiency, H=ca. 15 μm for a small alkylbenzene at u=0.3-0.4 mm/s in 70/30=acetonitrile/water, and slightly larger H for unretained uracil, were reported with K=0.63-0.82x10^{-14} m^2 for the TRIM monolith. Although correction for extra-column band broadening was included[164], and higher performance of monoliths with greater extent of crosslinking was shown, the net column efficiency was not very high. The positive effect of hypercrosslinking on column efficiency and permeability was also shown by Urban[165].

Preparation methods of hierarchically porous polymer monoliths were recently reported which include combination of control of macro- and micro-phase separation[166]. Polymer monolithic structures possessing macropores and mesopores were prepared based on controlled polymerization of styrene and divinylbenzene employing a poly(lactide) chain transfer agent in the presence of poly(ethylene oxide). Structural characterization indicated the presence of sub-micron macropores and mesopores (8-20 nm). The studies on chromatographic properties of these hierarchically porous monoliths will be of much interest, although the skeleton structures are supposed to be similar to those of conventional monoliths.

7.2.4 Organic-silica hybrid monolithic columns.

High efficiency columns have also been pursued with organic-inorganic hybrid monoliths prepared from alkoxysilane, siloxane, or polyhedral oligomeric silsesquioxanes (cage mixture,

POSS) as precursors for the inorganic portion. This review tentatively refers to this type of hybrid structure as an "organic-silica hybrid" as used also in some of the cited references. This section describes the development of organic-silica hybrid materials for the high-efficiency separation of small molecules in LC, while monoliths from mixed silanes were included in the silica monolith part.

Zajickova and coworkers optimized the preparation conditions of hybrid monoliths starting from 3-(methacryloyloxy)propyltrimethoxysilane[167,168]. The single monomer was polymerized in the presence of both 2,2-azobisisobutyronitrile and aqueous hydrochloric acid to form a polymeric stationary phase and siloxane structure simultaneously. The column efficiency, H=ca. 9 μm was obtained for benzene and toluene with retention factor k=ca. 1, at a linear velocity, u=ca. 0.3 mm/s. The monolith, however, showed a sharp increase in H at higher u, and with solutes with larger *k*, as commonly observed with polymer monolithic columns.

Polymer monoliths prepared by polymerization of monomers with silica precursors as a crosslinker by radical chain reactions could provide high efficiency, but phase separated structures have not been observed in the product so far, as shown above[167,168], or in other studies[169,170,171,172]. In contrast, several reports indicated that phase separated three dimensional network structures were obtained by step polymerization of modified siloxanes or modified POSS with monomers[173,174,175,176,177], or by a radical-mediated step-growth crosslinking reactions including vinyl-POSS and thiol components[178]. POSS may be regarded as a small silica unit in these reactions.

Zou and coworkers reported organic-silica hybrid monoliths prepared by epoxy-amine ring-opening polymerization of cyclosiloxane having two reactive groups, methacrylate and epoxy, as functional monomer with 1,10-diaminodecane was shown to possess bicontinuous network structure with ca. 2 μm through-pores and ca. 1 μm skeletons, while methacrylate-based free radical polymerization with ethylene dimethacrylate did not provide such a monolith structure[173].

Organic–silica hybrid monoliths prepared by a ring-opening polymerization of octaglycidyldimethylsilyl POSS (POSS-epoxy) with poly(ethylenimine) (PEI) possessed bicontinuous network structure consisting of through-pores and skeletons[174]. The monolith provided efficiency, H=9-10 μm for alkylbenzenes (benzene-butylbenzene) at u=0.7-1.1 mm/s independent of retention factor, for a range of k=0.3-1.5.

The reaction of POSS-epoxy with cystamine dihydrochloride resulted in a monolithic support having three dimensional skeleton morphology[175]. The disulfide linkage was reduced to give thiols, then used for the introduction of a hydrophobic stationary phase by the reaction with stearyl methacrylate or benzyl methacrylate via thiol-ene click reaction. The modification did not affect the column efficiency, which was shown to be H=ca. 14 μm, by preparing 100 cm column generating 70000 theoretical plates.

Thiol-ene click polymerization of methacrylate-POSS (POSS-MA) with multi-thiol crosslinkers, namely trimethylolpropane tris(3-mercaptopropionate), in the presence of porogenic solvents (n-propanol and PEG 200) and dimethylphenylphosphine, resulted in hybrid monolith with uniform through-pores of 1–2 μm and small skeletons of ~1 μm[176]. The monolithic column provided column efficiency, H=ca. 7-9 μm for alkylbenzenes in reversed-phase mode at 0.5-1 mm/s (minimum H=5.5 μm at 0.64 mm/s for butylbenzene with k=ca. 1.1), and efficiencies in the range of H=ca. 8-20 μm for polycyclic aromatic hydrocarbons, phenols, anilines, EPA 610 as well as bovine serum albumin (BSA) digest. The permeability was $K=1.01 \times 10^{-14}$ m^2 for a monolith with a large external porosity (e.g. 71.6%). In this example, alkylbenzenes showed increasing column efficiencies with increase in retention, a commonly observed tendency for silica-based columns, but the opposite to that typically found for organic monoliths.

Hybrid monoliths were prepared by thiol–epoxy click polymerization using POSS-epoxy and multi-thiol, PTM, to provide a high-efficiency organic-silica capillary column[177]. The monolith,

possessing phase separated bicontinuous structure (Figure 9A), generated H=ca. 5.5 μm for butylbenzene at u=0.8-1.0 mm/s with increasing efficiency with increasing retention. Thermal stability up to 300 ^{o}C, and pressure stability up to 40 MPa were mentioned.

Monolithic columns prepared by copolymerization of methacrylate epoxy cyclosiloxane and POSS-MA by photochemically initiated polymerization using a 1-propanol/PEG 400 mixture as porogens showed permeability K up to $2x10^{-14}$ m^2, and column efficiency, H=10 μm[171]. The efficiency was independent of retention factor up to 2.4 for alkylbenzenes, with linear velocity of mobile phase up to u=0.6 mm/s. Some monoliths prepared by photochemical initiation showed H=12-14 μm, with linear velocity up to u=1.4 mm/s without much increase in H. Using the same POSS-MA as silica precursor, phase separated morphology was not obtained in this case, although similar column efficiency was observed as with previous examples.

Alves and Nischang prepared organic-silica hybrid monoliths in 100 μm I.D. capillaries from vinyl-POSS and thiol component, 2,2'-(ethylenedioxy)diethanethiol, in porogenic co-solvent, THF and 1-dodecanol, by a radical-mediated step-growth crosslinking[178]. Structures of the monoliths produced under optimized conditions were bicontinuous as some silica monoliths (Figure 9B). The choice of the thiol monomer and its effectiveness in linking individual POSS units at an equimolar stoichiometry of functional groups were shown to be essential. The monolith provided plate height, H= ca. 10 μm, with little dependency on solute retention from t_0 up to k=ca. 20, and a small increase in H at higher linear velocity up to 2.2 mm/s with clear minimum at 0.2-0.5 mm/s. The permeability was $K=1.2x10^{-14}$ m^2 with total porosity of 84%. The column efficiency and permeability were dictated by the feature size. The monolith prepared in bulk did not show much surface area in the dry state. Similarity in chromatographic behavior between the monolith prepared in this study and that of silica monoliths was presented. Although HETP obtained with such a monolith is H=10-15 μm at present, consistent efficiency was obtained in 30/70 – 80/20 acetonitrile-water mobile phase.

7.2.5 Remarks on polymer monoliths and hybrid monoliths.

Polymer monoliths can now generate H= 5-10 μm with little increase with the retention factor of the solute. Their permeability is adequate for high-speed operation. For further improvement of column efficiency, one may need to improve the homogeneity of crosslinking density or gel structures that are solvated to different extents providing varying reduced mass transfer rate[179], and to understand the relation between the column efficiency and the presence of bicontinuous network structures produced by using POSS (Figure 9). It is commonly observed that high performance monoliths possess homogeneous phase separated structures. It should be critically examined whether the presence of a small silica unit as POSS is essential for high performance polymer monoliths or for phase separated structures. It will be of much interest to see whether organic-silica hybrid structures are stable against pressure and high flow rate as well as extreme pH conditions. The relation between morphology and column efficiency studied by serial block-face SEM may provide a key to future improvement of monolithic capillary columns[180].

It should be emphasized that high efficiency columns should be evaluated under practical conditions including adequate ranges of flow rate (up to 5 mm/s) and organic solvent content in combination with solutes having retention factors up to 5-10. Care should be taken to reduce extra-column band broadening for these measurements. Rigorous examination of pressure stability is also desirable. Because column efficiency seems to be so important for the research in this area, the performance of the new products should be shown with chromatograms including a peak for a column dead-volume marker with adequate information on experimental conditions including column dimensions, mobile phase composition and flow rate, and pressure, in addition to information on temperature, and the samples used for evaluation. Information on porosity, or the elution volume of the column dead-volume marker relative to empty column volume, may be discussed in relation to the porogen content of the preparation feed. With proper care in experiment and reporting, polymer monoliths will achieve the goal sooner with their flexible preparation methods studied by so many researchers.

8 Conclusion

This review documents some of the important developments that have taken place in the area of support materials for high performance liquid chromatography in recent years. Clearly, core-shell particles have become an important addition to the range of stationary phase supports, seeming to have few disadvantages compared with totally porous materials of the same particle size, while yielding higher efficiency. The reasons for this enhanced performance have been carefully explored, but some of the relevant issues, such as those concerning the influence of particle size distribution, have still not been fully resolved. The possibilities of slip flow, especially in capillary columns, have been investigated with a view to obtaining higher efficiencies with smaller particles at pressures lower than expected. Again, a full explanation of these interesting effects remains to be given. Monolithic silica columns still have the potential to rival particle packed columns in terms of high efficiency and low back pressure in many applications. Second generation materials, having higher homogeneity and synthesised with smaller through-pores and skeletons, have been shown to give improved efficiency. However, they unfortunately may sacrifice some of the benefits of the low operating pressures of the original columns. Provision of higher pressure-resistant cladding techniques for rod monoliths remains a goal. Organic polymer monoliths have remained important for the separation of biomolecules, while improvements have been made in their performance for small molecules. The development of organic monoliths has been supported by a sizeable research community, while relatively few researchers work on silica monoliths. New materials, such as pillar array columns, offer the promise of high performance separations in the future.

Biographies

Nobuo Tanaka is Professor Emeritus, Kyoto Institute of Technology, Japan, and currently working for GL Sciences, Inc. as an Advisor. He belongs to the honorary board of *Journal of Chromatography*. His research interests include monolithic silica columns, characterization and high-efficiency operation of small-size columns, and the effect of pressure on retention and selectivity in reversed-phase liquid chromatography.

David McCalley is Professor in Bioanalytical Science at the University of the West of England in Bristol, U.K. His research interests include liquid chromatography with small particles, the mechanism of reversed-phase and hydrophilic interaction separations, gas chromatography, coupled procedures with mass spectrometry, and applications of these techniques in the clinical, biomedical, pharmaceutical and environmental fields. He is a member of the Editorial Board of *Journal of Chromatography A* and acts as a referee for a number of other high –impact journals and grant-awarding bodies. He was named by Analytical Science magazine as one of the world's hundred most influential Analytical Scientists, both in 2013 and in 2015.

Acknowledgement

DM thanks Monika Dittman (Agilent Technologies, Waldbronn Germany) for providing some of the references for this work.

NT thanks Frantisek Svec (Lawrence Berkeley National Laboratory, Berkeley, USA), Attila Felinger, University of Pecs, Hungary), and Ulrich Tallarek (University of Marburg, Germany) for their helpful suggestions, Takeshi Hara (Institute of Physical Chemistry, Department of Chemical Engineering, Vrije University of Brussel) for supplying Figure 7, and Karin Cabrera (Merck, Darmstadt Germany) for supplying Figure 8A.

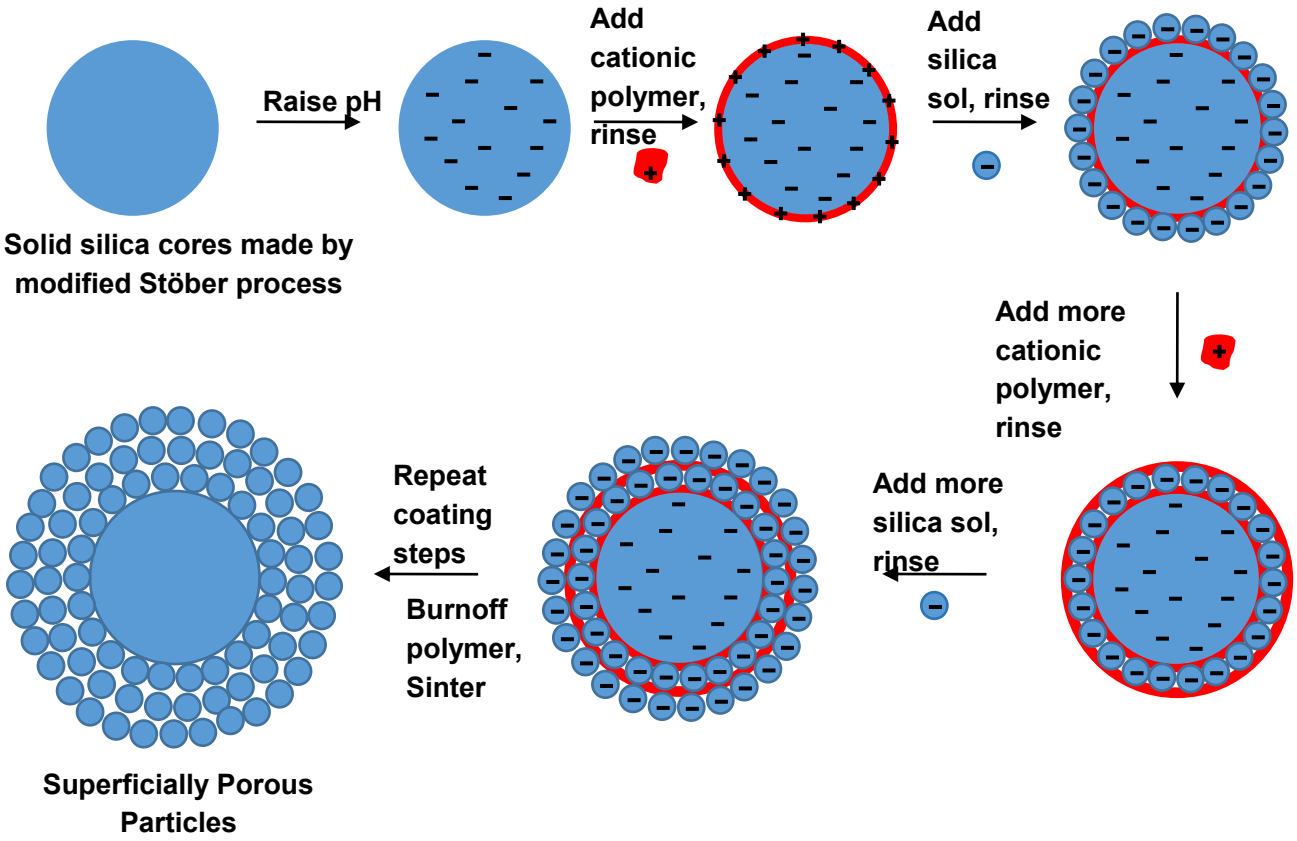

Urea, formaldehyde polymerization coats sol and core

Coated sol then adsorbs to coated core.

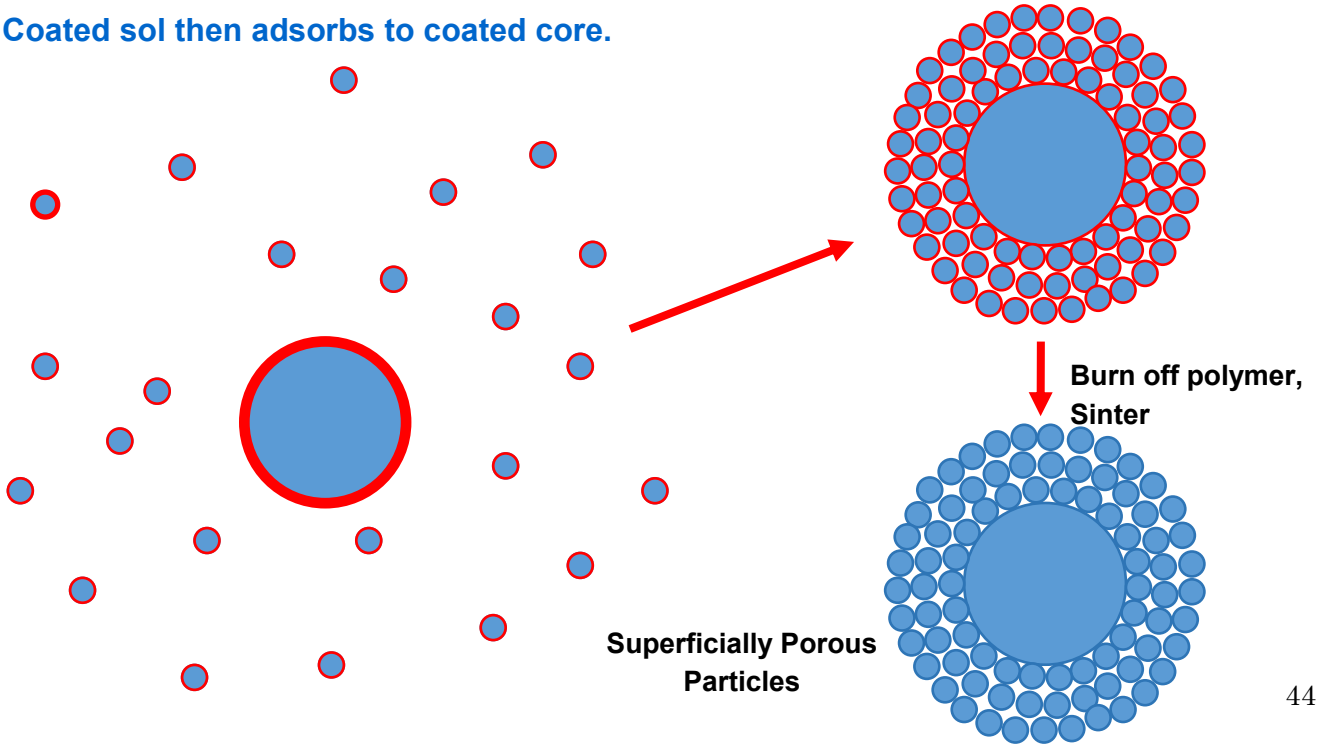

Fig. 1 a) Schematic of layer by layer process and b) schematic of modified coacervation method for synthesis of shell particles.

Reprinted from reference [20] *J. Chromatogr. A*, Vol. 1414, Chen, W.; Jiang, K.; Mack, A.; Sachok, B.; Zhu, X.; Barber, W. E.; Wang, X., Synthesis and optimization of wide pore superficially porous particles by a one-step coating process for separation of proteins and monoclonal antibodies., Pages 147-157, Copyright 2015, with permission from Elsevier.

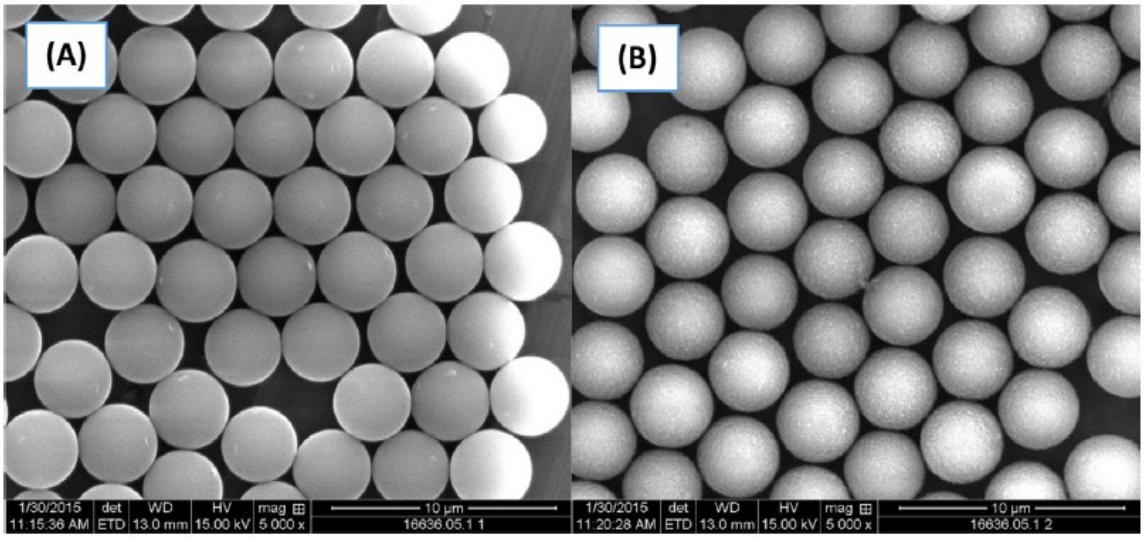

Fig. 2 Scanning electron micrographs of the carbon core (A) and finished material (B) of carbon based wide-pore nano diamond particles.

Reprinted from reference [29] *J. Chromatogr. A*, Vol. 1414, Fekete, S.; Jensen, D. S.; Zukowski, J.; Guillarme, D., Evaluation of a new wide-pore superficially porous material with carbon core and nanodiamond -polymer shell for the separation of proteins, Pages 51-59, Copyright 2015, with permission from Elsevier.

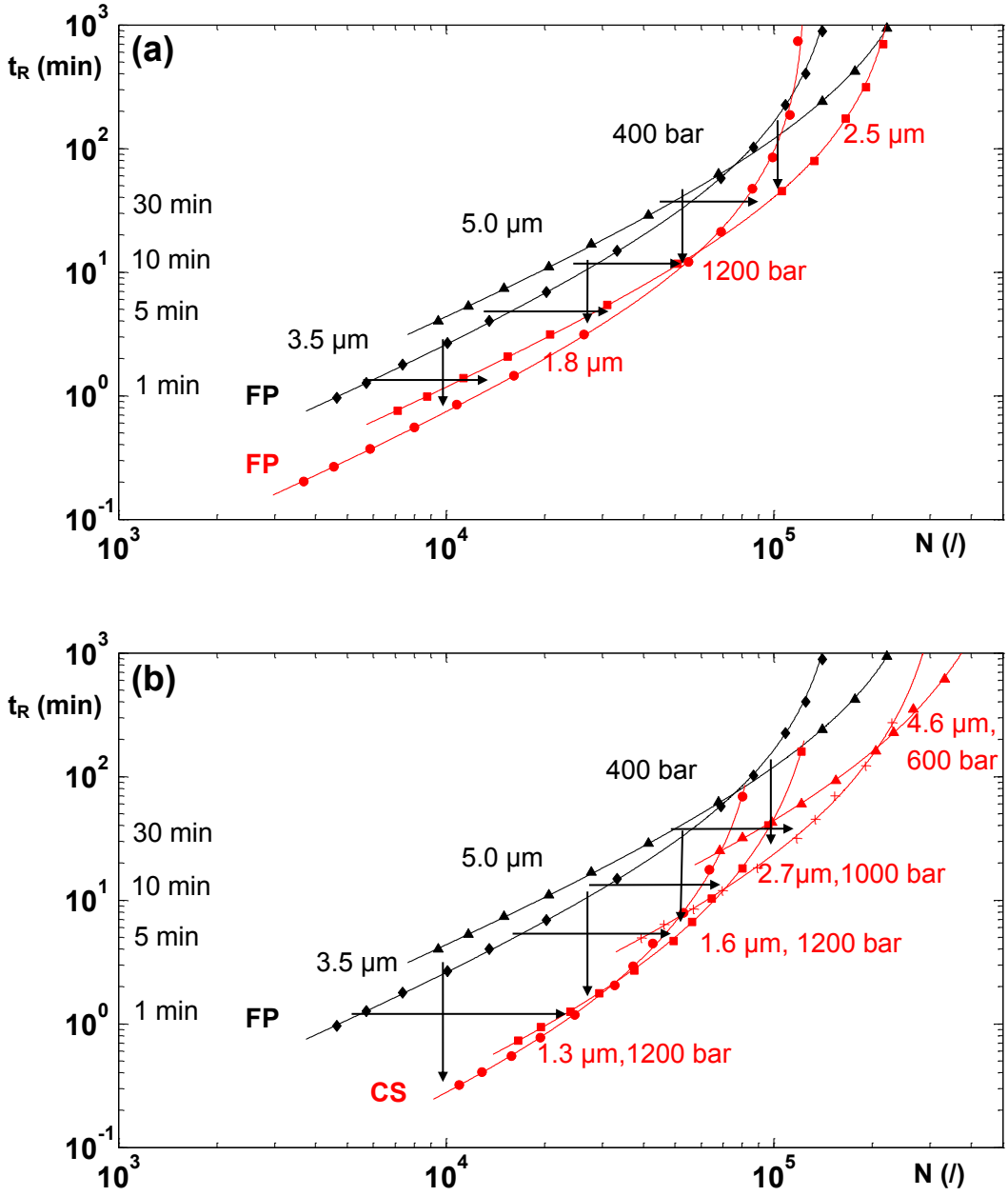

Fig 3 . Kinetic plots showing the progress (vertical and horizontal arrows) made recently for a) sub 2µm fully porous particles (red data) vs supra 2µm particles. b) inclusion of core shell columns. Plots are for small MW compounds, $k = 9$.

Reprinted from reference [30] *TrAC Trends in Analytical Chemistry*, Vol. 63, Broeckhoven, K.; Desmet, G., The future of UHPLC: Towards higher pressure and/or smaller particles?, Pages 65-75, Copyright 2014, with permission from Elsevier.

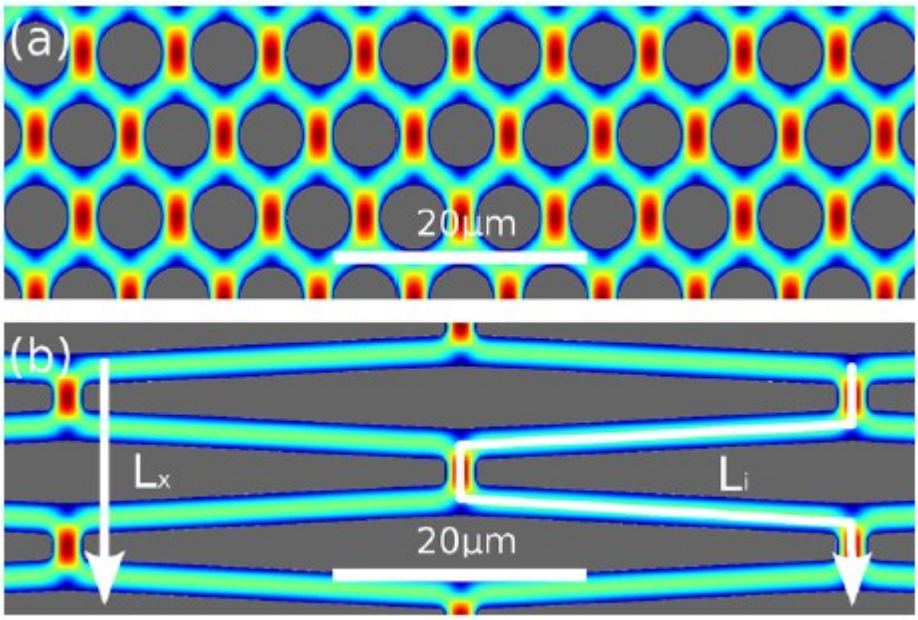

Fig 4 Top view of pillar arrangement and velocity field of (a) a conventional cylindrical pillar array column and (b) a radially elongated pillar column. The white arrow L_x indicates the net direction of flow; white arrow L_i indicates the direction of flow along the tortuous path followed by the liquid.

Reproduced from reference [96] Desmet, G.; Callewaert, M.; Ottevaere, H.; De Malsche, W. Anal. Chem. 2015, 87, 7382-7388. Copyright 2015 American Chemical Society.

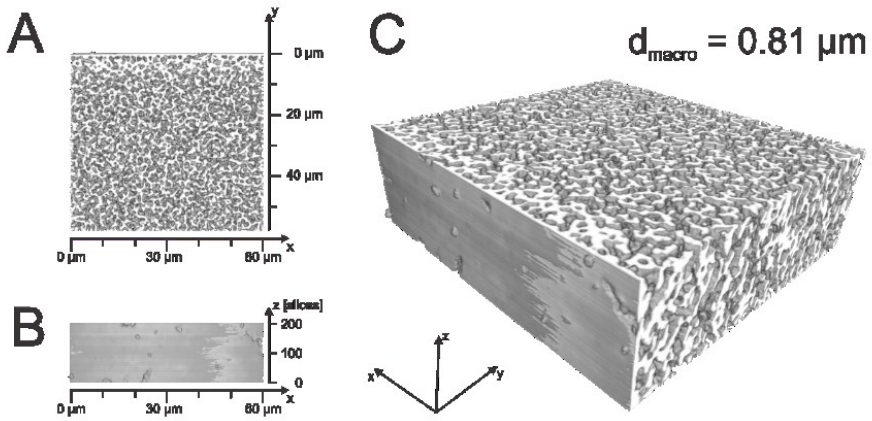

Figure 5. (A) CLSM-based reconstructed macropore space morphology of 2nd generation monoliths, representing a physical volume of about 60 µm × 60 µm × 25 µm (200 slices, C). The graphic features an x–y top view (A), an x–z side view (B), and a perspective representation (C) of the monolith reconstructions. The macroscopic boundary of silica rod is indicated by the ~1 µm thick silica layer at the origin of the y-axis.

Reprinted from reference [121], *J. Chromatogr. A* Volume 1312, Hormann, K.; Tallarek, U., Analytical silica monoliths with submicron macropores: Current limitations to a direct morphology–column efficiency scaling. Pages 26-36. Copyright 2013, with permission from Elsevier.

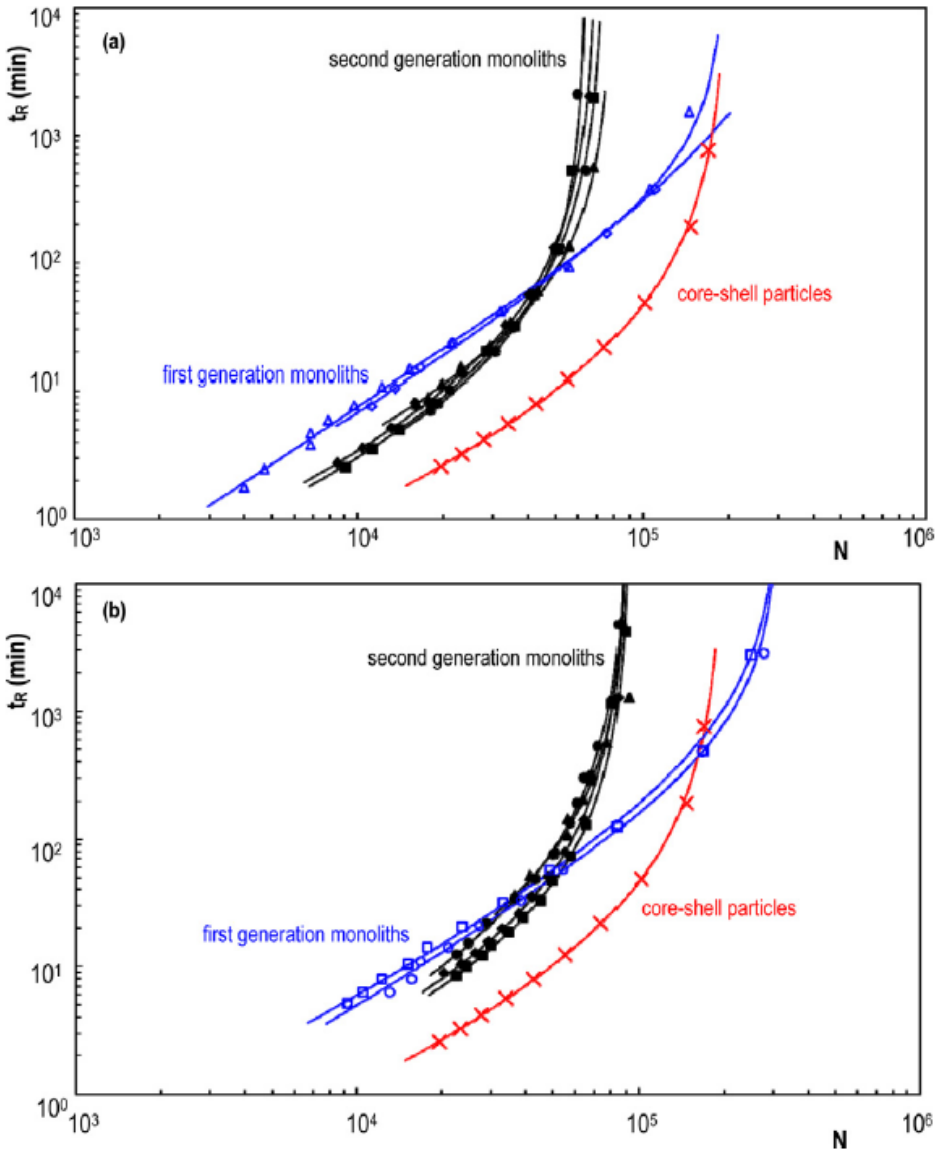

Figure 6. Kinetic plots of analysis time (t_R) vs plate count (N) for benzophenone for columns at 200 bar (a) monolith columns ID 2.0mm and (b) ID 3.0-3.2mm. Red curves are for a shell column (2mmx 100mm, d_p = 2.7 μm) operated at a maximum pressure of 600 bar.

Reprinted from reference [122], *J. Chromatogr. A* Volume 1325, Cabooter, D.; Broeckhoven, K.; Sterken, R.; Vanmessen, A.; Vandendael, I.; Nakanishi, K.; Deridder, S.; Desmet, G., Detailed characterisation of the kinetic performance of first and second generation silica monolithic columns for reversed-phase chromatography, Pages 72-82. Copyright 2014, with permission from Elsevier.

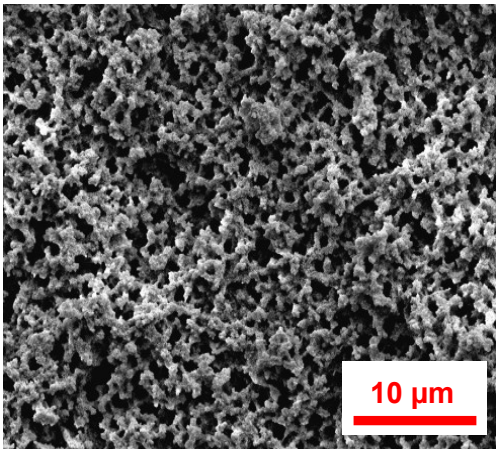

Figure 7. Scanning electron micrograph of a monolithic silica rod prepared with PEGs of MW = 20000. Reprinted from reference [127], Hara, T.; Desmet, G.; Baron, G. V.; Minakuchi, H.; Eeltink, S. Submitted to J. Chromatogr. A. Presented at 42nd International Symposium on High-Performance Liquid-Phase Separations and Related Techniques, June, 2015. Geneva, Switzerland. PSA-FUN-31. The figure was supplied by T. Hara.

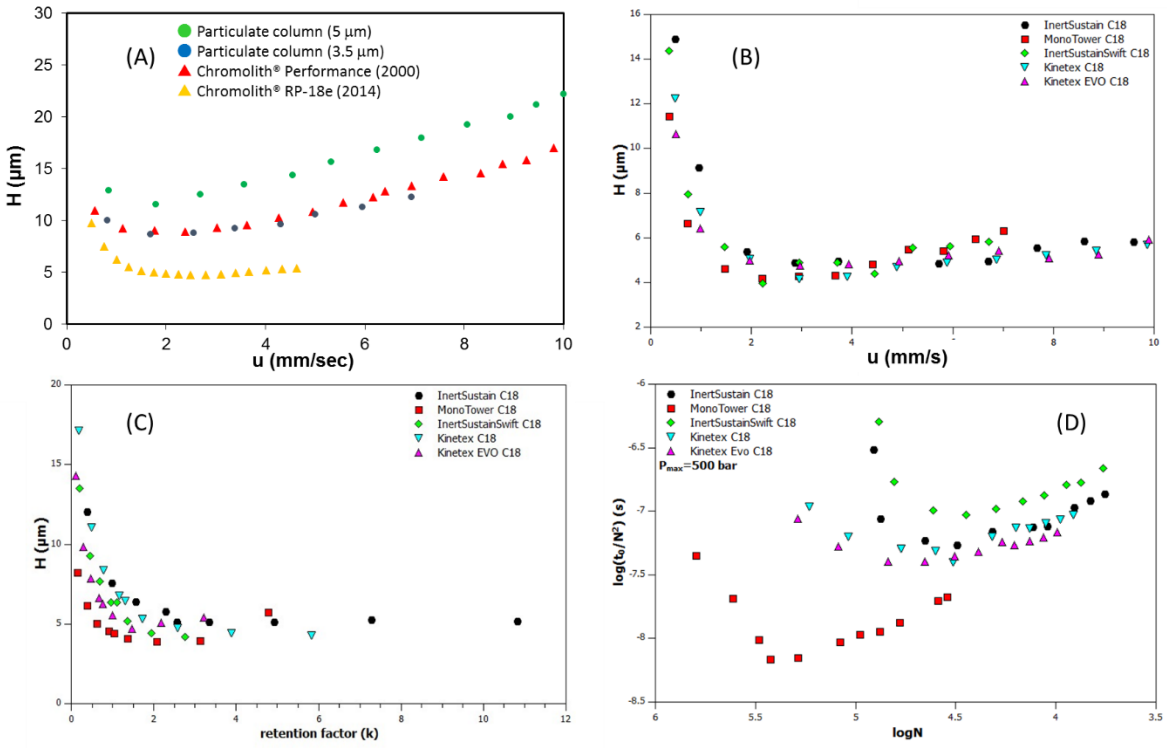

Figure 8. Performance of advanced silica columns. (A) Plot of plate height against linear velocity on Chromolith and particulate columns. The figure was supplied by K. Cabrera.

(B) Plot of plate height against linear velocity. Solute, heptanophenone. (C) Plot of the observed plate height against the retention factor of solutes (reversed-phase column performance test mixture containing acetanilide, acetophenone, propiophenone, butyrophenone, benzophenone, valerophenone, hexanophenne, heptanophenone, and octanophenone at 100 µg/mL each, in acetonitrile/water = 65/35, obtained from Agilent). (D) Kinetic plots based on the results with heptanophenone. Column, 2.1 mmID, 5 cm, 2 µm (InertSustain C18) and 1.9 µm (InertSustainSwift C18) totally porous particles, 2.6 µm core-shell particles (Kinetex C18 and Kinetex EVO C18), and for monolithic silica (MonoTower C18). Mobile phase, 65/35=acetonitrile/water. 40 ^{o}C. (B-D) Reprinted from reference 129. Lambert, N.; Felinger, A.; Miyazaki, S.; Ohira, M.; Tanaka, N. Submitted to *J. Chromatogr. A*. Presented at 10th Balaton Symposium on High-Performance Separation Methods, September, 2015. Siofok, Hungary. Poster – 49.

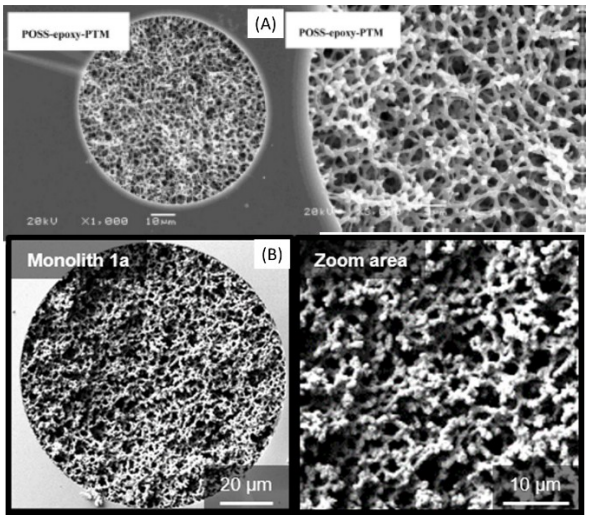

Figure 9. Scanning electron micrographs showing phase separated bicontinuous structures of organic-silica hybrid monoliths prepared from POSS derivatives.

(A) Reprinted from reference [177] *J. Chromatogr. A*, Volume 1416, Lin, H.; Chen, L.; Ou, J.; Liu, Z.; Wang, H.; Dong, J.; Zou, H. Preparation of well-controlled three-dimensional skeletal hybridmonoliths via thiol–epoxy click polymerization for highly efficient separation of small molecules in capillary liquid chromatography, Pages 74-82. Copyright 2015, with permission from Elsevier.

(B) Reprinted from reference [178], *J. Chromatogr. A,* Volume 1412, Alves, F.; Nischang, I. Radical-mediated step-growth: Preparation of hybrid polymer monolithic columns with fine control of nanostructural and chromatographic characteristics. Pages 112-125. Copyright 2015, with permission from Elsevier.

References

(1) Mazzeo, J. R.; Neue, U. D.; Kele, M.; Plumb, R. S. *Anal Chem* **2005**, *77*, 460a-467a.

(2) Cabrera, K.; Lubda, D.; Eggenweiler, H. M.; Minakuchi, H.; Nakanishi, K. *Hrc-J High Res Chrom* **2000**, *23*, 93-99.

(3) De Malsche, W.; De Beeck, J. O.; De Bruyne, S.; Gardeniers, H.; Desmet, G. *Anal Chem* **2012**, *84*, 1214-1219.

(4) Anon. *J Chromatogr A* **2014**, *1369*, 1-1.

(5) Adlard, E. R. *Chromatographia* **2015**, *78*, 1-1.

(6) Ainsworth, S. J. *Chem Eng News* **2015**, *93*, 32-33.

(7) Knox, J. H.; Saleem, M. *J. Chromatogr. Sci.* **1969**, *7*, 614-622.

(8) Halasz, I.; Endele, R.; Asshauer, J. *J Chromatogr* **1975**, *112*, 37-60.

(9) McCalley, D. V. *Trac-Trend Anal Chem* **2014**, *63*, 31-43.

(10) Horvath, C.; Preiss, B. A.; Lipsky, S. R. *Anal.Chem.* **1967**, *39*, 1422-1428.

(11) Kirkland, J. J.; Langlois, T. J.; DeStefano, J. J. *Am Lab* **2007**, *39*, 18-+.

(12) McCalley, D. V. *J Chromatogr A* **2011**, *1218*, 2887-2897.

(13) Hayes, R.; Ahmed, A.; Edge, T.; Zhang, H. *J Chromatogr A* **2014**, *1357*, 36-52.

(14) Gritti, F.; Guiochon, G. *J Chromatogr A* **2010**, *1217*, 1485-1495.

(15) Bell, D. S.; Henry, R. A.; Betz, W.; Ross, P. *Chromatography Today* **2015**, *8*, 34-37.

(16) Bell, D. S.; Majors, R. E. *Lc Gc N Am* **2015**, *33*, 386-+.

(17) Gonzalez-Ruiz, V.; Olives, A. I.; Martin, M. A. *Trac-Trend Anal Chem* **2015**, *64*, 17-28.

(18) Ruta, J.; Zurlino, D.; Grivel, C.; Heinisch, S.; Veuthey, J.-L.; Guillarme, D. *J Chromatogr A* **2012**, *1228*, 221-231.

(19) Stoeber, W.; Fink, A.; Bohn, E. *Jounal of Colloid and Interface Science* **1968**, *26*

62-69

(20) Chen, W.; Jiang, K.; Mack, A.; Sachok, B.; Zhu, X.; Barber, W. E.; Wang, X. *J Chromatogr A* **2015**, *1414*, 147-157.

(21) Kirkland, J. J.; Truszkowski, F. A.; Dilks, C. H.; Engel, G. S. *J Chromatogr A* **2000**, *890*, 3-13.

(22) Ahmed, A.; Forster, M.; Clowes, R.; Myers, P.; Zhang, H. F. *Chem Commun* **2014**, *50*, 14314-14316.
(23) Ahmed, A.; Hodgson, N.; Barrow, M.; Clowes, R.; Robertson, C. M.; Steiner, A.; McKeown, P.; Bradshaw, D.; Myers, P.; Zhang, H. F. *J Mater Chem A* **2014**, *2*, 9085-9090.
(24) Ahmed, A.; Myers, P.; Zhang, H. F. *Langmuir* **2014**, *30*, 12190-12199.
(25) Hayes, R.; Myers, P.; Edge, T.; Zhang, H. F. *Analyst* **2014**, *139*, 5674-5677.
(26) Deng, T. S.; Bongard, H. J.; Marlow, F. *Mater Chem Phys* **2015**, *162*, 548-554.
(27) Hung, C.-H.; Wiest, L. a.; Singh, B.; Diwan, A.; Valentim, M. J. C.; Christensen, J. M.; Davis, R. C.; Miles, A. J.; Jensen, D. S.; Vail, M. a.; Dadson, A. E.; Linford, M. R. *J Sep Sci* **2013**, *36*, 3821-3829.
(28) Bobály, B.; Guillarme, D.; Fekete, S. *Journal of Pharmaceutical and Biomedical Analysis* **2015**, *104*, 130-136.
(29) Fekete, S.; Jensen, D. S.; Zukowski, J.; Guillarme, D. *J Chromatogr A* **2015**, *1414*, 51-59.
(30) Broeckhoven, K.; Desmet, G. *TrAC Trends in Analytical Chemistry* **2014**, *63*, 65-75.
(31) Fekete, S.; Guillarme, D. *TrAC Trends in Analytical Chemistry* **2014**, *63*, 76-84.
(32) Perrenoud, A. G.-g.; Farrell, W. P.; Aurigemma, C. M.; Aurigemma, N. C.; Fekete, S.; Guillarme, D. *J Chromatogr A* **2014**, *1360*, 275-287.
(33) Fekete, S.; Guillarme, D. *J Chromatogr A* **2013**, *1308*, 104-113.
(34) Fekete, S.; Guillarme, D. *J Chromatogr A* **2013**, *1320*, 86-95.
(35) Dubbelman, A.-C.; Cuyckens, F.; Dillen, L.; Gross, G.; Hankemeier, T.; Vreeken, R. J. *J Chromatogr A* **2014**, *1374*, 122-133.
(36) Sanchez, A. C.; Friedlander, G.; Fekete, S.; Anspach, J.; Guillarme, D.; Chitty, M.; Farkas, T. *J Chromatogr A* **2013**, *1311*, 90-97.
(37) Bobály, B.; Guillarme, D.; Fekete, S. *J Sep Sci* **2014**, *37*, 189-197.
(38) Schuster, S. A.; Wagner, B. M.; Boyes, B. E.; Kirkland, J. J. *J Chromatogr A* **2013**, *1315*, 118-126.
(39) Vanderheyden, Y.; Cabooter, D.; Desmet, G.; Broeckhoven, K. *J Chromatogr A* **2013**, *1312*, 80-86.
(40) Kahsay, G.; Broeckhoven, K.; Adams, E.; Desmet, G.; Cabooter, D. *Talanta* **2014**, *122*, 122-129.

(41) Nishi, H.; Nagamatsu, K. *Analytical Sciences* **2014**, *30*, 205-211.

(42) Schuster, S. a.; Boyes, B. E.; Wagner, B. M.; Kirkland, J. J. *J Chromatogr A* **2012**, *1228*, 232-241.

(43) Vinci, G.; Antonelli, M. L.; Preti, R. *J Sep Sci* **2013**, *36*, 461-468.

(44) Gritti, F.; Guiochon, G. *J Chromatogr A* **2013**, *1280*, 35-50.

(45) Daneyko, A.; Hlushkou, D.; Barnau, V.; Khirevich, S.; Seidel-Morgenstern, A.; Tallarek, U. *J. Chromatogr. A* **2015**, *1497*, 139-156.

(46) Gritti, F.; Guiochon, G. *J Chromatogr A* **2012**, *1221*, 2-40.

(47) Gritti, F.; Guiochon, G. *J Chromatogr A* **2010**, *1217*, 8167-8180.

(48) Bruns, S.; Stoeckel, D.; Smarsly, B. M.; Tallarek, U. *J Chromatogr A* **2012**, *1268*, 53-63.

(49) Gritti, F.; Shiner, S. J.; Fairchild, J. N.; Guiochon, G. *J Chromatogr A* **2014**, *1334*, 30-43.

(50) Gritti, F.; Guiochon, G. *Anal Chem* **2013**, *85*, 3017-3035.

(51) Gritti, F.; Guiochon, G. *J Chromatogr A* **2012**, *1252*, 56-66.

(52) Gritti, F.; Guiochon, G. *J Chromatogr A* **2012**, *1252*, 31-44.

(53) Gritti, F.; Guiochon, G. *J Chromatogr A* **2012**, *1252*, 45-55.

(54) Horvath, K.; Lukacs, D.; Sepsey, A.; Felinger, A. *J Chromatogr A* **2014**, *1361*, 203-208.

(55) Gritti, F.; Bell, D. S.; Guiochon, G. *J Chromatogr A* **2014**, *1355*, 179-192.

(56) Gritti, F.; Guiochon, G. *J Chromatogr A* **2014**, *1355*, 164-178.

(57) Gritti, F.; Guiochon, G. *J Chromatogr A* **2015**, *1384*, 76-87.

(58) Gritti, F.; Guiochon, G. *J Chromatogr A* **2015**, *1392*, 10-19.

(59) Destefano, J. J.; Schuster, S. A.; Lawhorn, J. M.; Kirkland, J. J. *J Chromatogr A* **2012**, *1258*, 76-83.

(60) Min, Y.; Jiang, B.; Wu, C.; Xia, S.; Zhang, X.; Liang, Z.; Zhang, L.; Zhang, Y. *J Chromatogr A* **2014**, *1356*, 148-156.

(61) Fekete, S.; Berky, R.; Fekete, J.; Veuthey, J.-L.; Guillarme, D. *J Chromatogr A* **2012**, *1252*, 90-103.

(62) Wagner, B. M.; Schuster, S. a.; Boyes, B. E.; Kirkland, J. J. *J Chromatogr A* **2012**, *1264*, 22-30.

(63) DeStefano, J. J.; Boyes, B. E.; Schuster, S. A.; Miles, W. L.; Kirkland, J. J. *J Chromatogr A* **2014**, *1368*, 163-172.

(64) Langsi, V. K.; Ashu-Arrah, B. A.; Glennon, J. D. *J Chromatogr A* **2015**, *1402*, 17-26.

(65) Bacskay, I.; Sepsey, A.; Felinger, A. *J Chromatogr A* **2014**, *1339*, 110-117.

(66) Fallas, M. M.; Buckenmaier, S. M. C.; McCalley, D. V. *J Chromatogr A* **2012**, *1235*, 49-59.

(67) Gritti, F. *J Chromatogr A* **2015**, *1410*, 90-98.

(68) Buckenmaier, S.; Miller, C. A.; van de Goor, T.; Dittmann, M. M. *J Chromatogr A* **2015**, *1377*, 64-74.

(69) Bruns, S.; Franklin, E. G.; Grinias, J. P.; Godinho, J. M.; Jorgenson, J. W.; Tallarek, U. *J Chromatogr A* **2013**, *1318*, 189-197.

(70) Blue, L. E.; Jorgenson, J. W. *J Chromatogr A* **2015**, *1380*, 71-80.

(71) Novakova, L.; Vaast, A.; Stassen, C.; Broeckhoven, K.; De Pra, M.; Swart, R.; Desmet, G.; Eeltink, S. *J Sep Sci* **2013**, *36*, 1192-1199.

(72) Vaast, A.; Broeckhoven, K.; Dolman, S.; Desmet, G.; Eeltink, S. *J Chromatogr A* **2012**, *1228*, 270-275.

(73) Rogers, B. J.; Wei, B. C.; Wirth, M. *Lc Gc N Am* **2012**, *30*, 890-+.

(74) Wei, B. C.; Rogers, B. J.; Wirth, M. J. *J Am Chem Soc* **2012**, *134*, 10780-10782.

(75) Rogers, B. J.; Wirth, M. J. *Acs Nano* **2013**, *7*, 725-731.

(76) Rogers, B. J.; Birdsall, R. E.; Wu, Z.; Wirth, M. J. *Anal Chem* **2013**, *85*, 6820-6825.

(77) Yan, X. H.; Wang, Q. W. *J Sep Sci* **2013**, *36*, 1524-1529.

(78) Schure, M. R.; Maier, R. S.; Kroll, D. M.; Davis, H. T. *J Chromatogr A* **2004**, *1031*, 79-86.

(79) Wu, Z.; Rogers, B. J.; Wei, B. C.; Wirth, M. J. *J Sep Sci* **2013**, *36*, 1871-1876.

(80) Smits, W.; Deridder, S.; Desmet, G. *J Chromatogr A* **2014**, *1366*, 120-125.

(81) Wu, Z.; Wei, B. C.; Zhang, X. M.; Wirth, M. J. *Anal Chem* **2014**, *86*, 1592-1598.

(82) Rogers, B. A.; Wu, Z.; Wei, B. C.; Zhang, X. M.; Cao, X.; Alabi, O.; Wirth, M. J. *Anal Chem* **2015**, *87*, 2520-2526.

(83) Xiu, L. C.; Valeja, S. G.; Alpert, A. J.; Jin, S.; Ge, Y. *Anal Chem* **2014**, *86*, 7899-7906.

(84) Zhang, T. Y.; Quan, C.; Dong, M. W. *Lc Gc N Am* **2014**, *32*, 798-+.

(85) Lin, H. J.; Horvath, S. *Chem Eng Sci* **1981**, *36*, 47-55.

(86) Colon, L. A.; Cintron, J. M.; Anspach, J. A.; Fermier, A. M.; Swinney, K. A. *Analyst* **2004**, *129*, 503-504.

(87) Gritti, F.; Guiochon, G. *Chem Eng Sci* **2010**, *65*, 6310-6319.

(88) Grinias, J. P.; Keil, D. S.; Jorgenson, J. W. *J Chromatogr A* **2014**, *1371*, 261-264.

(89) Fekete, S.; Horvath, K.; Guillarme, D. *J Chromatogr A* **2013**, *1311*, 65-71.

(90) Fallas, M. M.; Tanaka, N.; Buckenmaier, S. M. C.; McCalley, D. V. *J Chromatogr A* **2013**, *1297*, 37-45.

(91) Okusa, K.; Iwasaki, Y.; Kuroda, I.; Miwa, S.; Ohira, M.; Nagai, T.; Mizobe, H.; Gotoh, N.; Ikegami, T.; McCalley, D. V.; Tanaka, N. *J Chromatogr A* **2014**, *1339*, 86-95.

(92) Heaton, J. C.; Wang, X. L.; Barber, W. E.; Buckenmaier, S. M. C.; McCalley, D. V. *J Chromatogr A* **2014**, *1328*, 7-15.

(93) Fekete, S.; Fekete, J.; Guillarme, D. *J Chromatogr A* **2014**, *1359*, 124-130.

(94) Fekete, S.; Guillarme, D. *J Chromatogr A* **2015**, *1393*, 73-80.

(95) He, B.; Tait, N.; Regnier, F. *Anal Chem* **1998**, *70*, 3790-3797.

(96) Desmet, G.; Callewaert, M.; Ottevaere, H.; De Malsche, W. *Anal Chem* **2015**, *87*, 7382-7388.

(97) De Beeck, J. O.; Callewaert, M.; Ottevaere, H.; Gardeniers, H.; Desmet, G.; De Malsche, W. *Anal Chem* **2013**, *85*, 5207-5212.

(98) De Beeck, J. O.; Callewaert, M.; Ottevaere, H.; Gardeniers, H.; Desmet, G.; De Malsche, W. *J Chromatogr A* **2014**, *1367*, 118-122.

(99) Song, Y.; Noguchi, M.; Takatsuki, K.; Sekiguchi, T.; Mizuno, J.; Funatsu, T.; Shoji, S.; Tsunoda, M. *Anal Chem* **2012**, *84*, 4739-4745.

(100) Song, Y.; Takatsuki, K.; Isokawa, M.; Sekiguchi, T.; Mizuno, J.; Funatsu, T.; Shoji, S.; Tsunoda, M. *Anal Bioanal Chem* **2013**, *405*, 7993-7999.

---

(101) Gritti, F.; Guiochon, G. *J. Chromatogr. A* **2012**, *1228*, 2-19.

(102) Motokawa, M.; Kobayashi, H.; Ishizuka, N.; Minakuchi, H.; Nakanishi, K.; Jinnai, H.; Hosoya, K.; Ikegami.; T. Tanaka, N. *J.Chromatogr. A*, **2002**, *961*, 53–63.

(103) Motokawa, M.; Ohira, M.; Minakuchi, H.; Nakanishi, K.; Tanaka, N. *J. Sep. Sci.* **2006**, *29*, 2471–2477.

(104) Tanaka, N.; Kobayashi, H.; Nakanishi, K.; Minakuchi H.; Ishizuka, N. *Anal. Chem*. **2001**, *73*, 420 A–429A.

(105) Guiochon, G. *J. Chromatogr. A* **2007**, *1168*, 101-168.

(106) Minakuchi H.; Nakanishi K.; Soga N.; Ishizuka N.; Tanaka N. *Anal. Chem*. **1996**, *68*, 3498-3501.

(107) Nakanishi, K.; Tanaka, N. *Acc. Chem. Res*. **2007**. *40*, 863-873.

(108) Desmet, G.; Clicq, D.; Gzil, P. *Anal. Chem*., **2005**, *77*, 4058–4070.

(109) Mriziq, K. S.; Abia, J. A.; Lee, Y. M.; Guiochon, G. *J. Chromatogr. A* **2008**, *1193*, 97-103.

(110) Hlushkou, D.; Hormann, K.; Höltzel, A.; Khirevich, S.; Seidel-Morgenstern, A.; Tallarek, U. *J. Chromatogr. A* **2013**, *1303*, 28-38.

(111) Soliven, A.; Foley, D.; Pereira, L.; Dennis, G. R.; Shalliker, R. A.; Cabrera, K.; Ritchie, H.; Edge, T.; *J. Chromatogr. A*, **2014**, *1334*, 16-19.

(112) Gzil, P.; Vervoort, N.; Baron, G. V.; Desmet, G. *Anal. Chem*. **2004**, *76*, 6707–6718.

(113) Hara, T.; Kobayashi, H.; Ikegami, T.; Nakanishi, K.; Tanaka, N. *Anal. Chem*. **2006**, *78*, 7632-7642.

(114) Morisato, K.; Miyazaki, S.; Ohira, M.; Furuno, M.; Nyudo, M.; Terashima, H.; Nakanishi, K. *J. Chromatogr. A* **2009**, 1216, 7384-7387.

(115) Hara, T.; Mascotto, S.; Weidmann, C.; Smarsly, B. M. *J. Chromatogr. A* **2011**, *1218*, 3624-3635.

(116) Cabrera, K. *LC–GC North Am*. **2012**, *30*, 30–35.

(117) Bacskay, I.; Sepsey, A.; Felinger, A. *J. Chromatogr. A* **2014**, *1359*, 112-116.

(118) Soliven, A.; Foley, D.; Pereira, L.; Pravadali-Cekic, S.; R. Dennis, G.; Cabrera, K.; Ritchid, H.; Edge, T.; Shalliker, R. A. *Microchem. J*. In Press, Available online 3 September **2015**.

(119) Gritti, F.; Guiochon, G. *J. Chromatogr. A* **2012**, *1227*, 82-95.

(120) Gritti, F.; Guiochon G. *J. Chromatogr. A* **2012**, *1225*, 79-90.

(121) Hormann, K.; Tallarek, U. *J. Chromatogr. A*, **2013**, *1312*, 26-36.

(122) Cabooter, D.; Broeckhoven, K.; Sterken, R.; Vanmessen, A.; Vandendael, I.; Nakanishi K.; Deridder, S.; Desmet, G. *J. Chromatogr. A* **2014**, *1325*, 72-82.

(123) Vaast, A.; Broeckhoven, K.; Dolman, S.; Desmet, G.; Eeltink, S. *J. Chromatogr.A*, **2012**, *1228*, 270-275.

(124) Fekete, S.; Veuthey, J.-L.; Guillarme, D. *J.Chromatogr. A*, **2015**, *1408*, 1-14.

(125) Diószegi, T. A.; Raynie, D. E. *J. Chromatogr. A*, **2012**, *1261*, 107-112.

(126) Broeckhoven, K.; Cabooter, D.; Eeltink, S.; Desmet G. *J. Chromatogr.A*, **2012**, *1228*, 20-30.

[127] Hara, T.; Desmet, G.; Baron, G. V.; Minakuchi, H.; Eeltink, S. Submitted to *J. Chromatogr. A*. Presented at 42nd International Symposium on High-Performance Liquid-Phase Separations and Related Techniques, June, 2015. Geneva, Switzerland. PSA-FUN-31.

(128) Cabrera, K.; Kupfer, T.; Jung, G.; Knoell, P.; Peters, B. Presented at 42nd International Symposium on High-Performance Liquid-Phase Separations and Related Techniques, June, 2015. Geneva, Switzerland. PSB-COL-03.

(129) Lambert, N.; Felinger, A.; Miyazaki, S.; Ohira, M.; Tanaka, N. Submitted to *J. Chromatogr. A*. Presented at 10th Balaton Symposium on High-Performance Separation Methods, September, 2015. Siofok, Hungary. Poster – 49.

(130) Ma, Y.; Chassy, A. W.; Miyazaki, S.; Motokawa, M.; Morisato, K.; Uzu, H.; Ohira, M.; Furuno, M.; Nakanishi, K.; Minakuchi, H.: Mriziq, K.; Farkas, T.; Fiehn, O.; Tanaka, N. *J. Chromatogr. A*, **2015**, *1383*, 47-57.

(131) Itoh, N.; Santa, T.; Kato, M. *J. Chromatogr. A* **2015**, *1404*, 141-145.

(132) Horie, K.; Kamakura, T.; Ikegami, T.; Wakabayashi, M.; Kato, T.; Tanaka, N.; Ishihama, Y. *Anal. Chem*. **2014**, 86, 3817–3824.

(133) Laaniste, A.; Marechal, A.; El-Debs, R.; Randon, J.; Dugas, V.; Demesmay, C. *J. Chromatogr. A* **2014**, *1355*, 296–300.

(134) El-Debs, R.; Marechal, A.; Dugas, V.; Demesmay, C. *J. Chromatogr. A* **2014**, *1326*, 89–95.

(135) Moravcová, D.; Haapala, M.; Planeta, J.; Hyötyläinen, T.; Kostiainen, R.; Wiedmer, S. K. *J. Chromatogr. A* **2014**, *1373*, 90-96

(136) Yang, P. L.; Zhou, Q. L.; Jia, L. *Anal. Methods*. 2013, 5, 3074–3081.

(137) Moravcová, D.; Planeta, J.; Wiedmer, S. K. *J. Chromatogr. A*. **2013**, *1317*, 159–166.

(138) Marechal, A.; Laaniste, A.; El-Debs, R.; Dugas, V.; Demesmay, C. *J. Chromatography A* **2014**, *1365*, 140-147.

(139) Soliven, A.; Dennis, G. R.; Hilder, E. F.; Shalliker, R. A.; Stevenson, P. G. *Chromatographia*. **2014**, 77, 663–671.

(140) Sancho, R.; Novell, A.; Svec, F.; Minguillón, C. *J. Sep. Sci.* **2014**, *37*, 2805–2813.

(141) Novell, A.; Minguillón, C. *J. Chromatogr. A*, **2015**, *1384*, 124-132.

(142) Forster, S.; Kolmar, H.; Altmaier, S. *J. Chromatogr. A*, **2013**, *1283*, 110-115.

(143) Forster, S.; Kolmar, H.; Altmaier, S. *J. Chromatogr. A*, **2013**, *1315*, 127-134.

(144) Qu, Q.; Liu, Y.; Shi, W.; Yan, C.; Tang, X. *J. Chromatogr. A*, **2015**, *1399*, 25-31.

(145) Svec, F.; Frechet, J. M. J. *Anal. Chem*. 1992, 64, 820-822.

(146) F.; Svec, Lv, Y. *Anal. Chem*. **2015**, *87*, 250–273.

(147) Svec, F. *J. Chromatogr. A* **2012**, *1228*, 250-262.

(148) Jandera, P. *J. Chromatogr. A* **2013**, *1313*, 37-53.

.

(149) Liu, K.; Aggarwal, P.; Lawson, J. S.; Tolley, H. D.; Lee, M. L. *J. Sep. Sci.* **2013**.*36*, 2767–2781

(150) Vaast, A.; Nováková, L.; Desmet, G.; de Haan, B.; Swart, R.; Eeltink, S. *J. Chromatogr. A.* **2013**, *1304*, 177–182.

(151) Vaast, A.; Terryn, H.; Svec, F.; Eeltink, S. *J. Chromatogr. A* **2014**, *1374*, 171-179.

(152) Nischang, I. *J. Chromatogr. A* **2014**, *1354*, 56-64.

(153) Rozenbrand, J.; van Bennekom W. P. *Chromatographia* **2013**, *76*, 1595-1602.

(154) Beneito-Cambra, M.; Herrero-Martínez, J. M.; Ramis-Ramos, G.; Lindner, W.; Lämmerhofer, M. *J.Chromatogr. A* **2011**, *1218*, 7275-7280.

(155) Vonk, R. J.; Aalbers, T.; Eeltink, S.; Schoenmakers, P. J. *J. Chromatogr.A* **2015**, *1401*, 60-68.

(156) Gritti, F.; Guiochon, G. *J. Chromatogr. A* **2014**, *1362*, 49-61.

(157) Nischang, I. *J. Chromatogr. A* **2012**, *1236*, 152-163.

(158) Laher, M.; Causon, T. J.; Buchberger, W.; Hild, S.; Nischang, I. *Anal. Chem*., **2013**, *85*, 5645–5649.

(159)Müllner, T.; Zankel, A.; Mayrhofer, C.; Reingruber, H.; Höltzel, A.; Lv, Y.; Svec, F.;

Tallarek, U. *Langmuir*, **2012**, *28*, 16733–16737.

(160) Aggarwal, P.; Asthana, V.; Lawson, J. S.; Tolley, H. D.; Wheeler, D. R.; Mazzeo, B. A.; Lee, M. L. *J. Chromatogr*. *A* **2014**, *1334*, 20-29.

(161) Liu, Z.; Ou, J.; Lin, H.; Wang, H.; Liu, Z.; Dong, J.; Zou, H. *Anal. Chem.*, **2014**, *86*, 12334–12340.

(162) Chen, L.; Ou, J.; Liu, Z.; Lin, H.; Wang, H.; Dong, J.; Zou, H. *J. Chromatogr. A* **2015**, *1394*, 103-110.

(163) Liu, K.; Aggarwal, P.; Tolley, H. D.; Lawson, J. S.; Lee, M. L. *J. Chromatogr. A* **2014**, *1367*, 90-98.
Fabrication of highly cross-linked reversed-phase monolithic columns via living radical polymerization-

(164) Aggarwal, P.; Liu, K.; Sharma, S.; Lawson, J. S.; Tolley, H. D.; Lee, M. L. *J. Chromatogr.A* **2015**, *1380*, 38-44.

(165) Janků, S.; Škeříková, V.; Urban, J. *J. Chromatogr. A* **2015**, *1388*, 151-157.

(166) S. A.; Saba, M. P. S.; Mousavi, P.; Bühlmann, M. A. Hillmyer, *J. Am. Chem. Soc.*, **2015**, *137*, 8896–8899.

(167) Weed A. M. K.; Dvornik, J.; Stefancin, J. J.; Gyapong, A. A.; Svec, F.; Zajickova, Z. *J. Sep. Sci.* **2013**, *36*, 270–278.

(168) Gharbharan, D.; Britsch, D.; Soto, G.; Weed, A.-M. K.; Svec, F.; Zajickova, Z. J. Chromatogr. A 2015, 1408, 101-107.

(169) Wang, H.; Ou, J.; Liu, Z.; Lin, H.; Peng, X.; Zou, H. *J. Chromatogr. A* **2015**, *1410*, 110-117.

(170) Zhang, H.; Ou, J.; Liu, Z.; Wang, H.; Wei, Y.; Zou, H. *Anal. Chem*. **2015**, *87*, 8789-8797.

(171) Shan, Y.; Qiao, L.; Shi, X.; Xu, G. *J. Chromatogr. A* **2015**, *1375*, 101-109.

(172) Xiong, X.; Yang, Z.; Li, Y.; Xiao, L.; Jiang, L.; Chen, Y.; Ma, M.; Chen, B. *J. Chromatogr. A* **2013**, *1304*, 85–91.

(173) Wang, H.; Ou, J.; Lin, H.; Liu, Z.; Huang, G.; Dong, J.; Zou, H. *J. Chromatogr. A* **2014**, *1367*, 131-140.

(174) Lin, H.; Ou, J.; Tang, S.; Zhang, Z.; Dong, J.; Liu, Z.; Zou, H. J. Chromatogr. A 2013, 1301, 131-138.

(175) Liu, Z. S.; Ou, J. J.; Lin, H.; Wang, H. W.; Dong, J.; Zou, H. F. *J. Chromatogr. A* **2014***, 1342*, 70–77.

(176) Lin, H.; Ou, J.; Liu, Z.; Wang, H.; Dong, J.; Zou, H. *J. Chromatogr. A* **2015**, *1379*, 34-42.

(177) Lin, H.; Chen, L.; Ou, J.; Liu, Z.; Wang, H.; Dong, J.; Zou, H. *J. Chromatogr. A* **2015**, *1416*, 74-82.

(178) Alves, F.; Nischang, I. *J. Chromatogr. A* **2015**, *1412*, 112-125.

(179) Causon, T. J.; Nischang, I. *J. Chromatogr. A* **2014,** *1358*, 165-171.

(180) Müllner, T.; Zankel, A.; Lv, Y.; Svec, F.; Höltzel, A.; Tallarek, U. *Adv. Mater*. **2015**, 1-5.

For Table of contents only